From the Klinik für Zahnärztliche Prothetik, Propädeutik und Werkstoffkunde

(Director: Prof. Dr. M. Kern)

at the University Medical Center Schleswig-Holstein, Campus Kiel

at Kiel University

Influence of adhesive technique and thermomechanical fatigue on the fracture strength of minimally invasive CAD/CAM occlusal veneers

Dissertation

to acquire the doctoral degree in dentistry (Dr. med. dent)

at the Faculty of Medicine

at Kiel University

presented by

Majed Al-Akhali

from Taiz

Kiel 2019

1st Reviewer: Prof. Dr. Matthias Kern

2nd Reviewer: Prof. Dr. Dr. Anton Dunsche

Date of oral examination: 16.12.2019

Approved for printing, Kiel,

Signed:

(Chairperson of the Examination Committee)

CONTENTS

ABBREVIATIONS

Abbreviation	Description
○	Degree
BIS-GMA	Bisphenol A-glycidyl methacrylate
C	Centigrade
CAD/CAM	Computer-aided design and computer-aided manufacturing
CEJ	Cementoenamel junction
FDPs	Fixed dental prostheses
GPa	Gigapascal
HEMA	2-Hydroxyethylmethacrylate
Hz	Hertz
J	Joule
Kg	Kilogram
LED	Light-emitting diode
LiS_2	Lithium disilicate
min	Minute
mm	Millimeter
µm	Micrometer
MPa	Megapascal
N	Newton
PMMA	Polymethylmethacrylate
sec	Second
STL	Standard triangle language
TMD	Temporomandibular disorder
ZrO_2	Zirconia

1. INTRODUCTION

A loss of occlusal contacts between mandibular and maxillary teeth may result from pathological or functional problems such as tooth wear and caries [41] or an open posterior occlusal relationship with or without orthodontic therapy. Resulting dental problems may include a reduction of masticatory efficiency, loss of vertical dimension, hypersensitivity, and discoloration [30,69]. Under these circumstances, occlusal glass-ceramic veneers may provide a conservative prosthetic solution [30,84]. However, the space for an occlusal restoration might be limited by tooth compensated eruption [94] which may require removal of tooth structure and exposure of dentin [31,94]. As a result of losing the benefit of superior bond to the enamel tissue, the long-term vitality and survivability of the teeth as well as the fracture strength of the tooth and restoration may be adversely affected [22,31,39,74]. Fortunately, restorative dental materials with improved fracture strength have been introduced for use in minimal thicknesses [9,34,56]. Furthermore, improved dental adhesive systems in terms of mechanical, physical, and optical properties, allow dentists to use more conservative restorative approaches [13].

1.1. Polymer restorations

Resin based restorative materials are often based on bis-acryl (Bis-GMA) or polymethylmethacrylate (PMMA) [19]. The use of polymer-based restorative materials for long-term indirect restorations has been expanded [44,66] as a consequence of the significant and rapid improvements in the dental materials' properties over the last decade [36,50]. Studies showed that resin-based restorative materials were successfully used not only as direct but also as indirect restorative materials [44,65,78]. However, they are mainly recommended to be used as interim restorations in dentistry as their wear resistance is limited [8]. Nevertheless, the mechanical properties of these materials are within the acceptable range for fabrication a single dental restoration and the fracture strength of indirect composite resin crowns, inlays, and onlays were comparable to ceramic ones [18,44,56,88].

In general, polymerization of CAD/CAM polymers in industry is carried out with standardized high pressure and temperature, resulting in a higher degree of conversion with less residual monomers as compared to conventional polymers, this is considered as an advantage with regard to biocompatibility and long-term stability [30], but considered a disadvantage regarding bonding to luting resins [51,92]. The mechanical and physical properties of industrial polymerized CAD/CAM polymer restorative materials have been continually improved to be

used as an alternative to glass-ceramics, especially when thin restorations with high masticatory loads are required because of their high resistance to dynamic fatigue [63,64,84].

Mange et al. [63] and Schlichting et al. [84] evaluated the fatigue resistance of different materials as occlusal veneers in stepwise loading from 200 N to 1,400 N for a total of 185,000 cycles. They found that polymer-based materials had significantly increased fatigue resistance when compared to lithium disilicate. However, polymer-based materials have limitations for use as definitive restorations, including wear, discoloration, and low fracture strength which may allow clinicians to use them as long-term provisional restorations [30,84].

1.2. Glass-ceramic restorations

Ceramics are defined as non-metallic, inorganic, solid made objects, formed by baking raw materials (minerals) at high temperature [24,70,80]. According to the chemical composition, dental ceramics can be classified into three categories: 1) silicate ceramics, which could be further differentiated into feldspathic porcelain and glass-ceramics such as lithium disilicate ceramic; 2) non-silicate or high strength oxide-ceramics such as zirconia or alumina; 3) non-oxide ceramics such as nitrides and carbides [15,70]. The latter are not used in dentistry due to their inadequate esthetic appearance [85].

High strength glass- and oxide-ceramic materials have shown promising outcomes in terms of survival rate, integrity, wear resistance, and color stability when used as complete or partial-coverage crowns, veneers, inlays, onlays, and 3-unit fixed dental prostheses (FDPs) [6,21,39,47,82,98]. Lithium disilicate ceramic has been considered the strongest glass-ceramic restorative material. The high number of microstructural, interlocking, needle-like lithium disilicate crystals that are embedded in the glassy matrix gives this type of ceramic better mechanical properties than other types of glass-based ceramic materials [71]. Lithium disilicate ceramic has an average flexural strength of 530 MPa [2], fracture toughness of 2.5-3 $MPa \cdot m^{0.5}$ [38], and a modulus of elasticity of 95 GPa for both machinable (IPS e.max CAD) and pressable form (IPS e.max Press). Lithium disilicate ceramic has the esthetic and mechanical capability to be used as monolithic restorative material to restore anterior and posterior teeth with single restorations and up to 3-unit FDPs [47,52,100].

In the oral environment, restorative materials are subjected to many deteriorating factors, such as fatigue [40], wear [3], and/or erosion [79]. Therefore, restorative materials restoring the occlusal surface should meet the mechanical requirements for high-stress bearing posterior

restorations [12]. Up to now zirconia is considered the strongest and toughest restorative dental ceramic material, with a flexural strength of 900–1,400 MPa and a fracture toughness of 5-10 $MPa \cdot m^{0.5}$ [67]. The microstructure of restorative materials plays the most important role in determining their mechanical properties [28]. Dental manufacturers continually develop improved restorative materials to overcome the destructive oral challenges. Tooth morphology [53], restoration design [39,76], and thickness [39,82] are affecting the survivability and fracture strength of the restorative material and the tooth itself. Dissolving zirconia into the lithium silicate glass matrix claimed to be more translucent and stronger material than conventional lithium disilicate ceramic [34]. Therefore, zirconia approx. 10 wt% reinforced lithium silicate glass-ceramic material (Vita Suprinity, Vita Zahnfabrik; Celtra Duo, DENTSPLY) was developed in cooperation with Degudent GmbH and the Fraunhofer Institute for Silicate Research ISC. According to the manufacturer, dissolving of 10% zirconia into the lithium silicate glass matrix results in 4 times smaller silicate crystals, implying a high glass content and higher translucency than conventional lithium disilicate ($LiSi_2$) ceramic [8]. According to the manufacturer, this material has a flexural strength of 420 MPa, fracture toughness of 2 $MPa \cdot m^{0.5}$, and modulus of elasticity of 70 GPa.

Some laboratory studies showed that resin bonded occlusal veneers made of glass-ceramic materials with a non-retentive design had the capability to withstand 600,000 thermodynamic loading cycles [22,82]. Also when the thickness was reduced from 2 mm to 0.5 mm occlusally using pressed lithium disilicate, the restorations survived 1.2 million loading cycles. In addition, this reduction of thickness did not impair the fracture resistance of occlusal onlays [39]. A study by Clausen et al. [22] investigated the fracture strength of CAD/CAM lithium disilicate occlusal veneers with fissure/cusp thicknesses of 1.5/2 mm bonded to enamel using the etch-and-rinse bonding technique. They reported that all specimens survived the 600,000 thermodynamic loading cycles and recorded a fracture strength of 4,156 N. Likewise, Sasse et al. [82] evaluated the fracture strength of CAD/CAM lithium disilicate occlusal veneers with a variation of fissure/cusp thicknesses of 0.3/0.6 mm, 0.5/0.8 mm, and 0.7/1 mm bonded to enamel using a self-etch bonding system (Multilink primer A/B; Ivoclar Vivadent AG). As a result, they found that the survival rates after the 600,000 thermodynamic loading cycles of the different thicknesses were 50%, 75%, and 100%, and the median fracture strengths were 610 N, 2,355 N, and 2,070 N, respectively. Guess et al. [39], measured the fracture strength of retentive occlusal onlays made from pressed lithium disilicate bonded to teeth by the etch-and-rinse bonding technique. They

recorded median fracture strengths of 979 N and 1,055 N for occlusal onlays with thicknesses of 0.5 mm and 1 mm, respectively. A laboratory study by Yildiz et al. [98], evaluated the fracture strength of partial coverage crowns made from machinable lithium disilicate ceramic with an occlusal thickness of 1.5 mm. They recorded a higher fracture strength of 1,584.1 ±237.9 to 2,356 ±677 N for self-etch and etch-and-rinse bonding technique, respectively. Another laboratory study [54] restored molars of 2 mm occlusal reduction with different indirect restorative materials. Here lithium disilicate partial coverage restorations had a significantly higher mean fracture resistance of 2,522 N than feldspathic ceramic, leucite-reinforced ceramic, and resin-based composite materials.

1.3. Indirect composite restorations

As an attempt to improve the mechanical and the optical properties of glass-ceramic materials, new composite ceramic products have been developed for CAD/CAM technology. These composite ceramics were introduced as competitive substitutes for the traditional machinable ceramics.

Based on the glass infiltrated ceramic technique, a ceramic network structure is infiltrated with a polymer material (Vita Enamic; Vita Zahnfabrik) as a trying to combine the advantages of the two materials with the aim to obtain better mechanical properties in terms of weibull modulus and better machinability for CAD/CAM than those of glass-ceramics [23,42,68]. Some authors [23,26,42] showed that the infiltration of polymer phase into the feldspathic ceramic phase could provide a material with acceptable mechanical properties to be used as a permanent single tooth restoration. The fabrication of this material requires two processes, a porous pre-sintered ceramic network is produced and conditioned by a silane coupling agent; and then, this network is infiltrated with a polymer by capillary action [23]. Vita Enamic has a flexural strength of 140-160 MPa [23,56], a fracture toughness of 1 $MPa \cdot m^{0.5}$ [26], and a modulus of elasticity of 30 GPa [42,56].

In contrast, a resin nano ceramic (Lava Ultimate, 3M ESPE) formulated using nanomer particles from silica and zirconia treated with silane coupling agent to bond chemically to the resin matrix, has a flexural strength of 204 ±19 MPa, a fracture toughness of 2 $MPa \cdot m^{0.5}$, and a modulus of elasticity of 12.8 MPa [4,9,58]. In June 2015, 3M ESPE posted on its website that due to the higher debonding rate of crowns, the crown indication was withdrawn for this material. Today, the manufacturer indicates Lava Ultimate only for inlays, onlays, and veneers anymore.

A laboratory study [43] evaluated the fracture strength of two composite occlusal veneers (Lava Ultimate and Paradigm MZ100) with different thicknesses of 0.3, 0.6, and 1 mm. High fracture strengths for both tested materials ranged from 1,620 N to 2,141 N. Different thicknesses had no statistically significant effect on fracture strength in this study.

1.4. Bonding techniques

Adhesive luting is supporting the tooth structures and has a great consequence on the longevity of non-metallic restorations by increasing retention, fracture strength, and marginal adaptation of the restorations [11,55,73], especially with minimally invasive non-retentive preparations located within the enamel [73] and dentin [97]. This is especially beneficial in situations of compromised retention and high occlusal loads [14-16].

The adequate method of roughening and increasing the surface area of the bonding surfaces of the restorations depends on the prosthetic restorative material itself. Oxide-ceramic and industrially polymerized CAD/CAM resin-based restorations need to be abraded with airborne-particles [59], while glass-ceramic restorations require etching with 5% hydrofluoric acid for 20-60 sec depending on the included quantity of the glass phase [22]. Recently, a new single-component ceramic primer has been introduced to the dental market, which is composed of a blend of a ceramic conditioner and a silane coupling agent in one bottle (Monobond Etch & Prime; Ivoclar Vivadent AG). Laboratory studies [29,33,61,96] found that the surface treatment of glass ceramics with the self-etching primer (Monobond Etch & Prime) resulted in comparable bond strength results to hydrofluoric acid etching and using a primer containing silane separately. Otherwise, zirconia treated with air-borne-particle abrasion followed with self-etching primer provided statistically significantly lower bond strength than when air abrasion was followed by a universal primer application (Monobond Plus) [96].

Several bonding techniques and systems have been introduced to the dental market with the aim to achieve a durable bond to both, enamel and dentin [10,20]. Bonding techniques can be classified as etch-and-rinse (total-etch) and self-etching protocols [77]. Etch-and-rinse adhesive systems use 30% to 40% phosphoric acid to create a porous enamel surface to be penetrated by bonding resin tags [87]. Self-etching adhesive systems that contain monomers with grafted carboxylic or phosphate acid groups function by etching and penetrating the tooth substance simultaneously [25], and they were developed to simplify the adhesive bonding steps, save time, and reduce postoperative sensitivity when used on dentin [83].

An etch-and-rinse adhesive system can be offered as a three-steps system consisting of etching, priming, and bonding, or two-steps system where primer and bonding resin are mixed in one component [25]. In contrast, self-etch adhesives are either two-steps system involving the application of a solution containing non-rinse acidic primer followed by bonding resin, or they are more simplified one-step "all-in-on" systems [60,91]. Using self-etch adhesive seems to be beneficial for dentin, as it leaves a substantial amount of hydroxyapatite crystals around the collagen fibrils, which is considered an important factor in the durability of the bond [25]. Some studies [35,95] reported that the self-etch adhesive technique is not sufficient to obtain a porous enamel surface, thus, pre-application of phosphoric acid on enamel prior to self-etch adhesives is advisable to achieve a durable bond. However, up to now the three-step etch-and-rinse adhesives in combination with dual-curing luting resin remain the "gold standard" for adhesive systems in terms of durability [25,83].

Adhesively luted non-retentive dental restorations with etch-and-rinse bonding technique on enamel withstood the thermomechanical fatigue loading equivalent to 5 years of clinical fatigue and yielded high fracture strength values [22,39]. Thin conservative occlusal veneers were advantageous when adhesively bonded to enamel, which offers higher bond and fracture strengths when compared to veneers bonded to dentin [22,62,72,84]. Ma et al. [62] concluded that the load-bearing capacity of thin lithium disilicate occlusal veneers and onlays becomes less sensitive to its thickness when bonded to enamel. Likewise, Bindl et al. [13] stated that adhesive luting balanced the strength of weak ceramics with that of strong ceramic. However, a recent study of Yazigi et al. [97] evaluated the efficiency of immediate dentin sealing and different bonding protocols on the fracture resistance of lithium disilicate occlusal veneers with a thickness of 0.8 mm at cusps and 0.5 mm at fissures. Their results showed that immediate dentin sealing resulted in significantly higher fracture strength regardless of the bonding protocols or the artificial aging, recording fracture strengths ranging from 1,122 N to 1,853 N.

Limited and conflicting scientific data are available on the use and durability of different available CAD/CAM restorative materials as occlusal veneers with reduced thickness [22,39,43,63,82,84,97]. Moreover, data regarding the influence of different enamel etching techniques and thermomechanical fatigue on the fracture strength of the non-retentive design of dental restorations are sporadic. Direct comparison of different enamel etching technique, thermomechanical loading, and different types of CAD/CAM materials is missing in the

literature. Furthermore, data of zirconia-reinforced lithium silicate and polymer-infiltrated ceramics for this indication as occlusal veneers are missing.

2. AIM OF THE STUDY

The aim of this study was to evaluate the influence of thermomechanical loading and adhesive luting techniques on the fracture strength of minimally invasive thin occlusal veneer restorations fabricated from four different dental CAD/CAM materials: lithium disilicate, zirconia-reinforced lithium silicate, polymer-infiltrated ceramic, and polymethylmethacrylate PMMA.

The null hypothesis of this study was that the different tested CAD/CAM materials, bonding techniques, and thermomechanical loading will not influence the fracture strength of the tested occlusal veneers.

3. MATERIALS AND METHODS

3.1. Test groups

Study design and group codes are illustrated in Fig. 1 and Table 1. The compositions and batch numbers of the main materials used in this study are presented in Table 2.

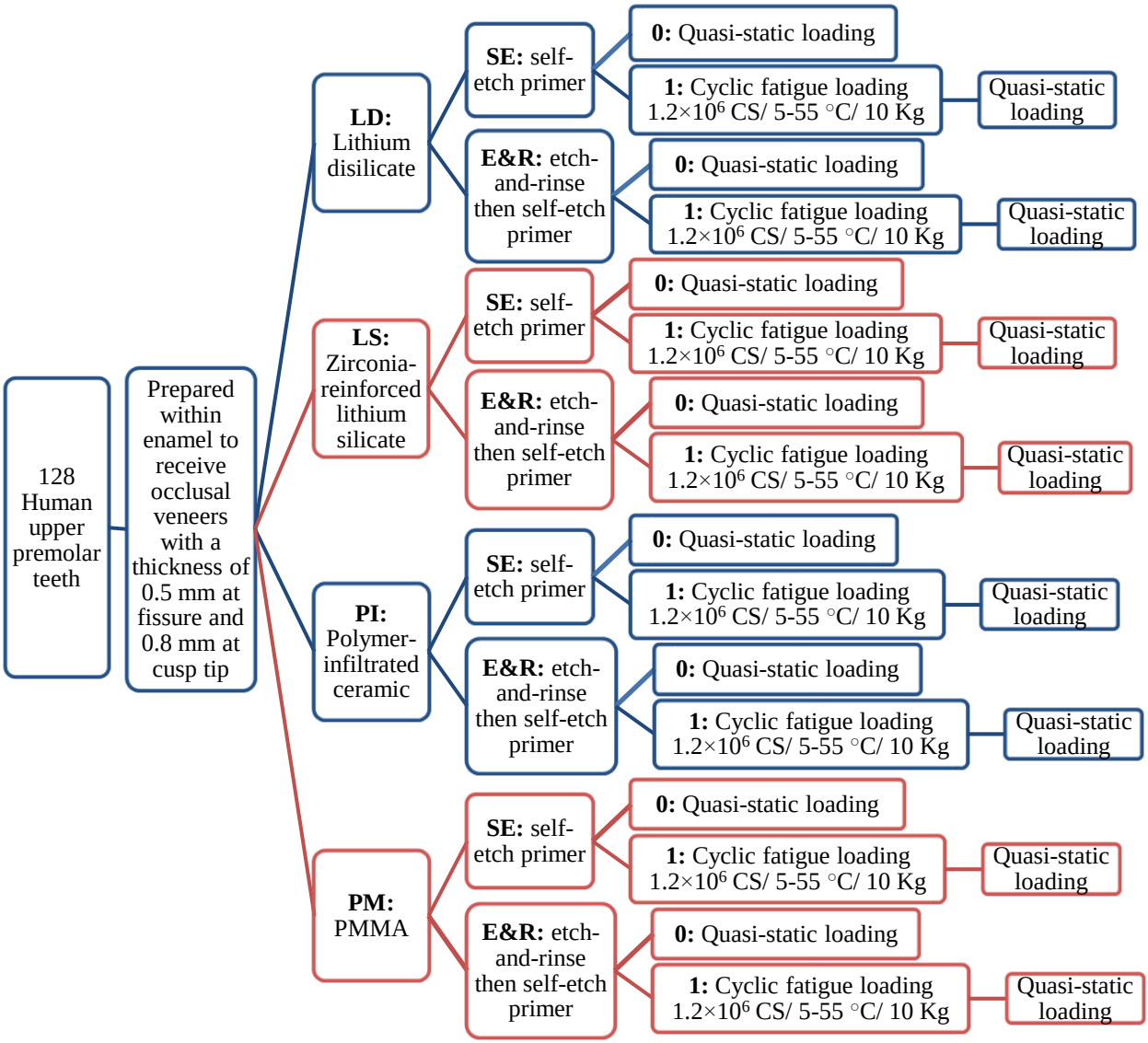

Fig. 1. Flow chart of study design

Two hundred intact, noncarious, unrestored human maxillary first premolars, recently extracted for orthodontic reasons, were collected anonymously. They were cleaned from both calculus deposits and soft tissues, and then they were stored at room temperature in 0.1% thymol solution (Caelo, Hilden, Germany). The teeth in this study were selected to be as similar as possible in dimension. Therefore, the mesiodistal and buccolingual as well as the buccal and lingual cusp slopes of the tooth occlusal surfaces were measured and determined as 5.4 ±0.7 mm, 5.7 ±0.6 mm, 4.2 ±0.5 mm, and 3.2 ±0.3 mm, respectively. Hence, teeth below or above the average ±SD were excluded from the study. Finally, a total of 128 teeth were selected for the purpose of this study.

Table 1. Study design and group codes (n=8)

CAD/CAM material (n=32)	**Etching technique (n=16)**	**Without thermomechanical loading (n=8)**	**After thermomechanical loading (n=8)**
Lithium disilicate (LD)	Self-etch (SE)	LD-SE-0	LD-SE-1
	Etch-and-rinse (E&R)	LD-E&R-0	LD-E&R-1
Zirconia-reinforced lithium silicate (LS)	Self-etch (SE)	LS-SE-0	LS-SE-1
	Etch-and-rinse (E&R)	LS-E&R-0	LS-E&R-1
Polymer-infiltrated ceramic (PI)	Self-etch (SE)	PI-SE-0	PI-SE-1
	Etch-and-rinse (E&R)	PI-E&R-0	PI-E&R-1
Polymethylmethacrylate PMMA (PM)	Self-etch (SE)	PM-SE-0	PM-SE-1
	Etch-and-rinse (E&R)	PM-E&R-0	PM-E&R-1

All teeth were fixed within copper metallic brass tubes (Ø 15 mm) so that the exposed root portions were coated 2 mm apical to the cementoenamel junction (CEJ) with 0.2 mm thick artificial periodontal membrane made from a gum resin (Anti-Rutsch-Lack; Wenko-Wenselaar,

Hilden, Germany). Subsequently, an autopolymerizing resin (Technovit 4000; Kulzer, Wehrheim, Germany) was used to fix the coated roots inside the metallic brass tubes.

For the purpose of fixing each tooth within the copper metallic brass tube, the CEJ of the tooth was determined and marked with a permanent marker. Then the tooth was oriented with its longitudinal axis inside a copper metallic brass tube 22 mm length, 15 mm outer diameter, and 13 mm inner diameter, and the empty space between the root and the inner side of the metallic brass tubes was filled with wax (Surgident Periphery Wax; Kulzer) up to 2 mm apical to the CEJ (Fig. 2.a). A dual-mixed phase single-stage impression technique with putty and light-bodied vinyl polysiloxanes material (Virtual; Ivoclar Vivadent AG, Schaan, Liechtenstein) was used (Fig. 2.b). The tooth crown and part of the metallic brass tube were impeded inside the impression mold, and the tube and wax were removed to expose root 2 mm apical to the CEJ, so that the exposed root portion was coated 2 mm apical to the CEJ with 0.2 mm thick artificial periodontal membrane made from a gum resin (Anti-Rutsch-Lack; Wenko-Wenselaar). The uniform coating allowed tooth mobility similar to the physiological mobility of the natural teeth [7,46,52]. Finally, an empty metallic brass tube was fitted on the impression mold (Fig. 2.c), and subsequently, an autopolymerizing resin (Technovit 4000; Kulzer), which simulated the human alveolar bone [22], was used to fix the coated root inside the metallic brass tube. As a result, the autopolymerizing resin flowed exactly 2 mm apical to the CEJ all around the tooth (Fig. 2.d). During polymerization of the autopolymerizing resin, specimens were stored in tap water to avoid a thermal impact of the exothermic reaction on the specimens [22].

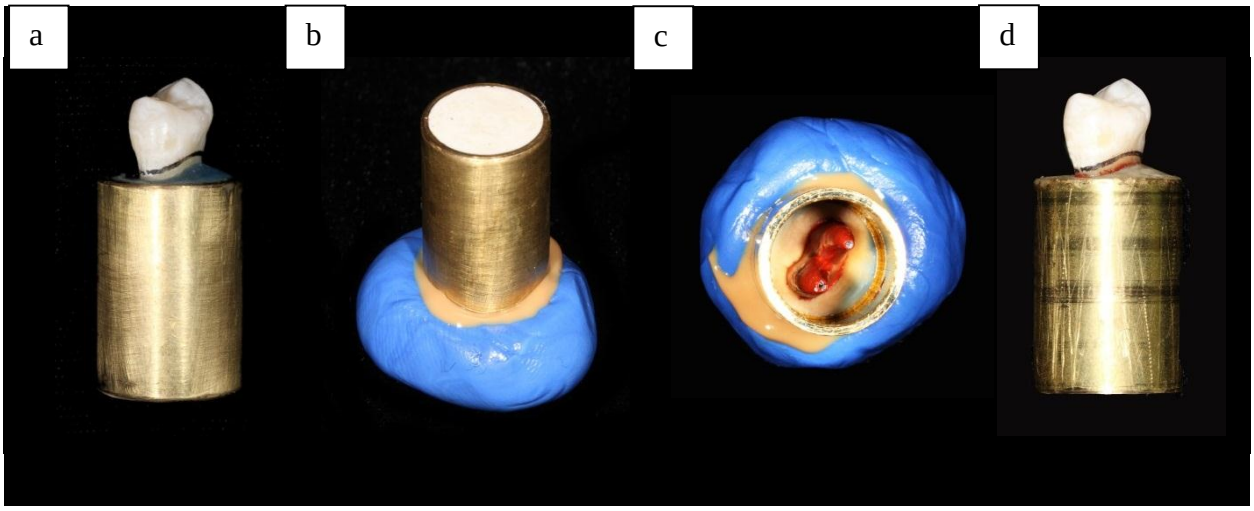

Fig. 2. a. Wax as a mold, b. Impression making for the wax mold, c. new metallic brass fitted on the impression, d. Autopolymerizing resin replacing the wax

Table 2. Materials used in this study

Commercial name of Material	Description	Company	Batch no
IPS e.max CAD	Lithium disilicate glass-ceramic blocks	Ivoclar Vivadent AG	T33444
VITA SUPRINITY	10 wt% zirconia reinforced lithium silicate glass-ceramic blocks	VITA Zahnfabrik	36852
VITA ENAMIC	14 wt% polymer infiltrated ceramic network hybrid blocks	VITA Zahnfabrik	100019
Telio CAD	Acrylate polymer (PMMA) blocks	Ivoclar Vivadent AG	T02661
Universal Adhesive	Universal Adhesive for siloxane impression materials	Kulzer	400463
Virtual, Putty	Polyvinylsiloxane impression material	Ivoclar Vivadent AG	SL4193
Virtual, Light body	Polyvinylsiloxane impression material	Ivoclar Vivadent AG	SL4086
IPS Ceramic Kit (Etching gel)	Hydrofluoric acid gel 5%	Ivoclar Vivadent AG	S48776
Monobond Plus	Universal primer: Alcohol solution of silane methacrylate, phosphoric acid methacrylate and sulphide methacrylate	Ivoclar Vivadent AG	S49812
Luxatemp Glaze & Bond	PMMA primer: Multifunctional acrylates, methyl methacrylate, catalysts, stabilizers, additives	DMG	715291
Total etch	Etching gel 37% phosphoric acid	Ivoclar Vivadent AG	S53647
Multilink Primer A and B	Primer A: an aqueous solution of initiators. Primer B: HEMA, phosphonic acid and methacrylate monomers	Ivoclar Vivadent AG	T04945
Multilink Automix	Dual-curing adhesive luting resin. The monomer matrix is composed of dimethacrylate and HEMA. The inorganic fillers include barium glass, ytterbium trifluoride and spheroid mixed oxide.	Ivoclar Vivadent AG	T03802
IPS e.max CAD Crystall./Glaze (paste)	Lithium disilicate Crystall./Glaze (paste)	Ivoclar Vivadent AG	T28633
VITA AKZENT PLUS	Suprinity/Glaze (paste)	VITA Zahnfabrik	43590
VITA ENAMIC GLAZE	Enamic/Glaze (liquid)	VITA Zahnfabrik	53570
Standard straight fissure diamond bur	ISO 806 314 158524 012	Komet Dental	428100
Fine straight fissure diamond bur	ISO 806 314 158514 012	Komet Dental	131353

3.2. Tooth preparation

A handpiece attached to a custom-made paralleling machine and a 120-degree angulated adaptor were used to prepare the teeth using a serial of straight fissure diamond burs under profuse water cooling (#837KR.314.012, #8837KR.314.012; Komet Dental, Brasseler GmbH & Co, Lemgo, Germany). The occlusal surfaces of the teeth were prepared within the enamel layer with the following standardized preparation criteria: 120-degree was the angle between the buccal and lingual cusp slopes, mesiobuccal and distobuccal slopes, mesiolingual and distolingual slopes, and finishing line and lingual cusp slope, with all angles rounded (Fig. 3). The prepared teeth were randomly assigned by running the function "RAND" in Excel software (Excel 2013; Microsoft Corp) into 4 groups (n=32), according to the restorative CAD/CAM materials used in the study.

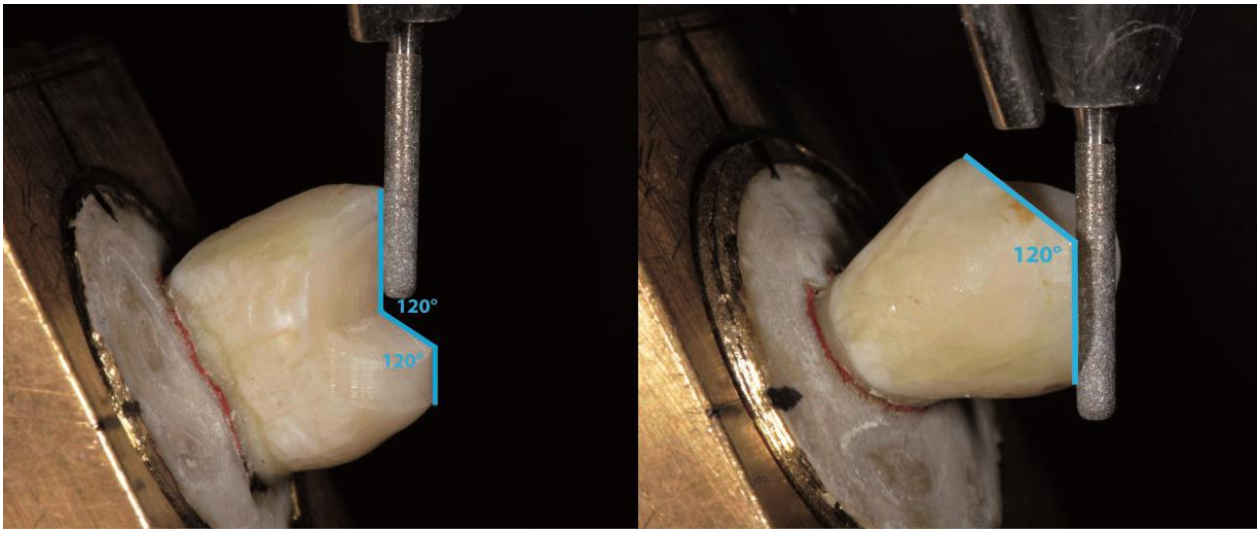

Fig. 3. Occlusal surface preparation with 120-degree between the prepared surfaces

3.3. Impression taking

A custom-made device and special tray were used for impression taking. Impressions were done using dual-mixed impression technique with putty and light-bodied vinyl polysiloxane materials (Virtual; Ivoclar Vivadent AG) and universal adhesive for siloxane impression materials (Universal Adhesive; Kulzer). The impressions were poured in Type IV stone (New Fujirock; GC, Alsip, IL, USA) to form working dies (Fig. 4). A 3D scanner (D900 3D scanner;

3shape, Copenhagen, Denmark) was used to scan the stone die and create a virtual model (Fig. 5). After that the occlusal veneers were designed virtually.

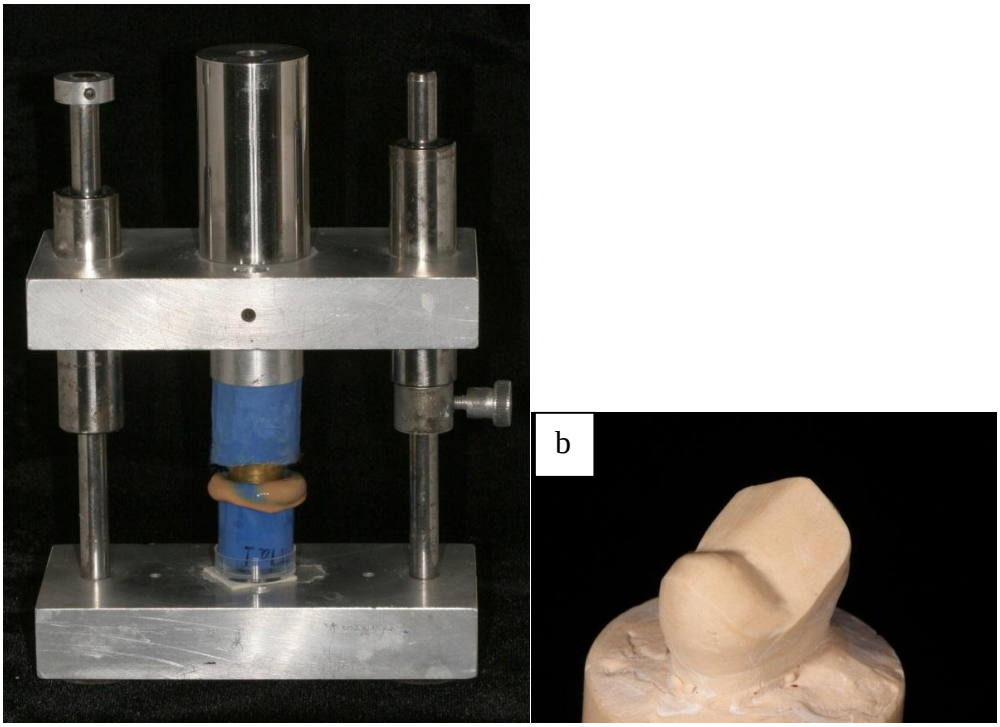

Fig. 4. a. Impression taking for a prepared specimen and b. working die

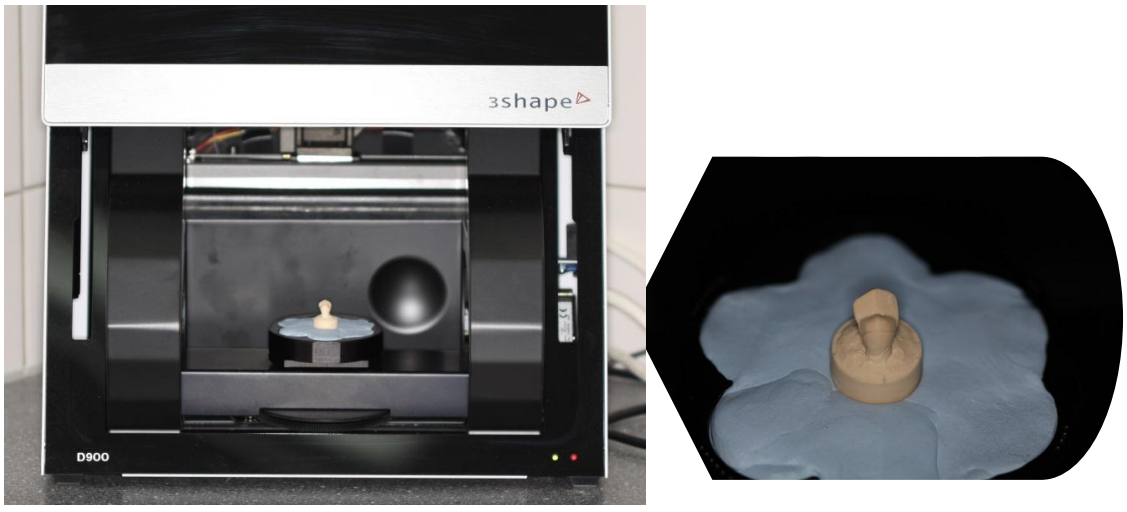

Fig. 5. 3D scanner

3.4. Restoration fabrication

The occlusal veneer restorations were designed in CAD-software (Dental Designer-Premium 2013; 3Shape) with thicknesses of 0.5 mm at the fissures and 0.8 mm at the cusps (Fig. 6).

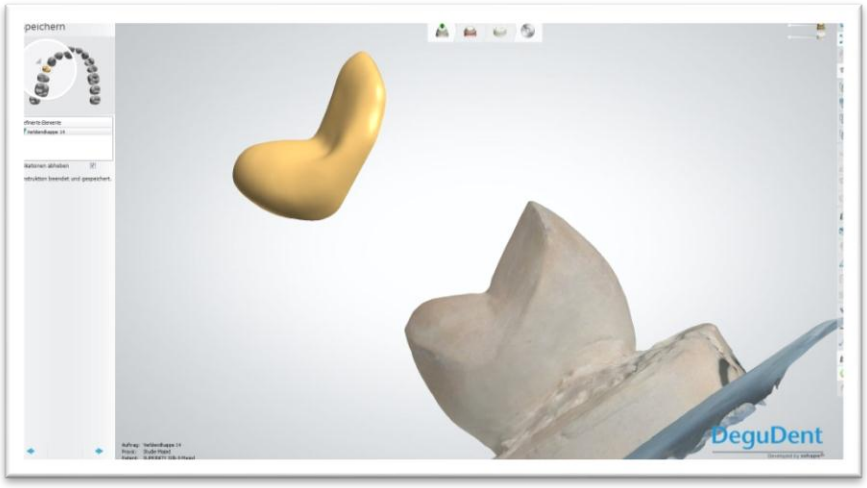

Fig. 6. Virtual design of an occlusal veneer

The virtual data were transferred in standard triangle language (STL) format to the milling machine software (inLab 3D software V3.10; Sirona). Milling sprue locations were designated on the distal surface of each final proposal. Thereafter, restorations were fabricated with a milling machine (inLab MC XL; Sirona, Bensheim, Germany) from four different CAD/CAM materials: group LD lithium disilicate ceramic (e.max CAD; Ivoclar Vivadent AG), group LS zirconia-reinforced lithium silicate ceramic (Vita Suprinity; Vita Zahnfabrik, Bad Säckingen, Germany), group PI polymer-infiltrated ceramic (Vita Enamic; Vita Zahnfabrik), and group PM polymethylmethacrylate (PMMA) (Telio CAD; Ivoclar Vivadent AG) as shown in Figs. 7 and 8. Finally, the thickness of all milled restorations was checked using a caliper (Praecimeter; Renfert, Hilzingen, Germany) and adjusted manually if needed using a straight fissure diamond bur (#8837KR.314.012; Komet Dental) under water coolant (Fig. 9). After the milling procedure and the presumable manual adjustment of thicknesses, occlusal veneers were cleaned with water steam (Fig. 10).

Fig. 7. CAD/CAM blocks used in the study

Fig. 8. Milled occlusal veneer restoration (VITA SUPRINITY; Vita Zahnfabrik)

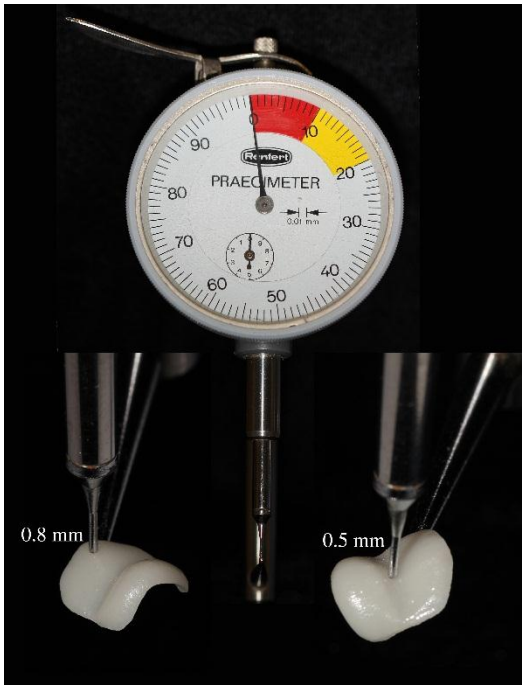

Fig. 9. Checking the occlusal veneer thicknesses

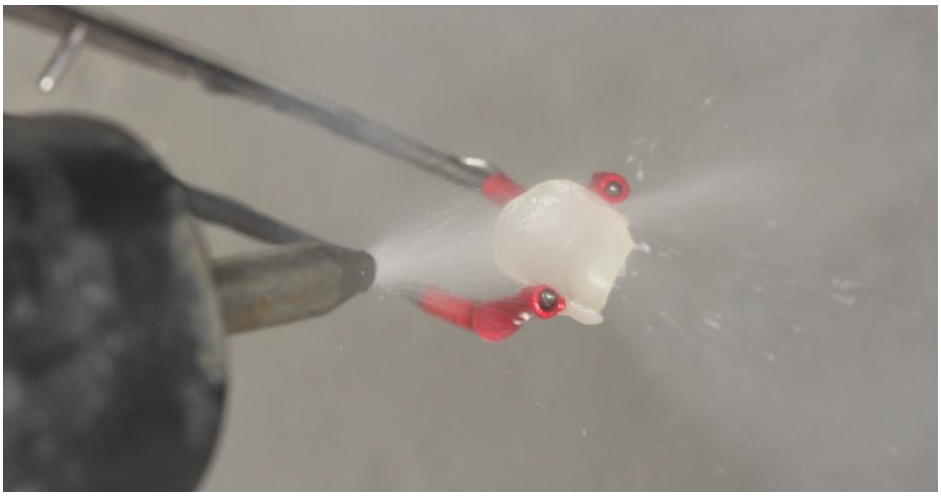

Fig. 10. Water steam cleaning of a milled occlusal veneer

Corresponding glazes (e.max CAD glaze paste; Ivoclar Vivadent AG) and (Vita Akzent plus glaze paste; Vita Zahnfabrik) were used for e.max CAD and Vita Suprinity, respectively. Then a combination firing (crystallization and glaze firing) was carried out in one-step using a furnace (Programat EP 5000; Ivoclar Vivadent AG) according to the manufacturers' instructions. Vita Enamic was glazed with Vita Enamic glaze (Vita Zahnfabrik) and polymerized in a light

polymerization unit (UniXS Kulzer; Kulzer) for 10 min. Telio CAD was polished according to the manufacturer's instructions. Finally, the finished occlusal veneers, with their respective prepared teeth in every group (n=32/group), were randomly assigned into 2 subgroups (n=16/subgroup) according to the enamel conditioning method, either self-etching or etch-and-rinse (Figs. 11 and 12).

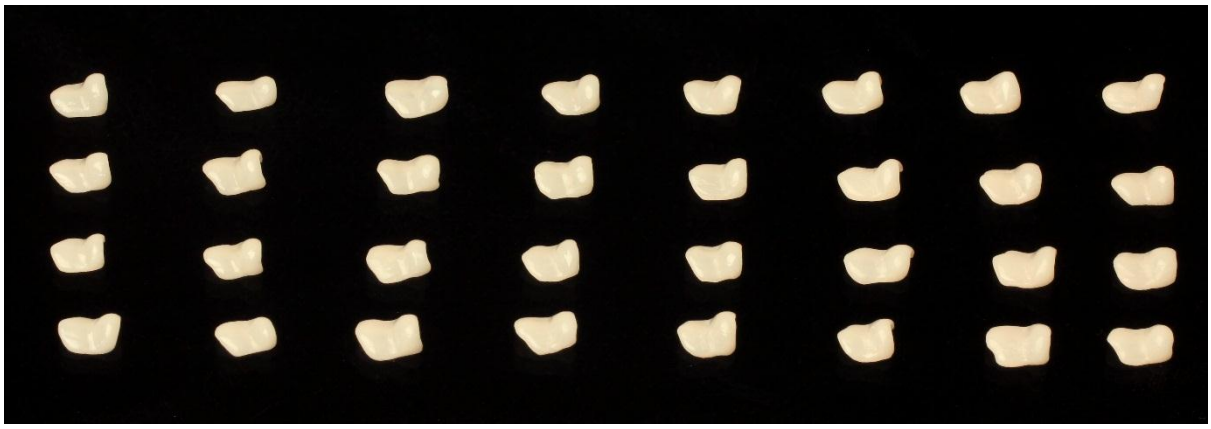

Fig. 11. Finished occlusal veneer restorations from Telio CAD material

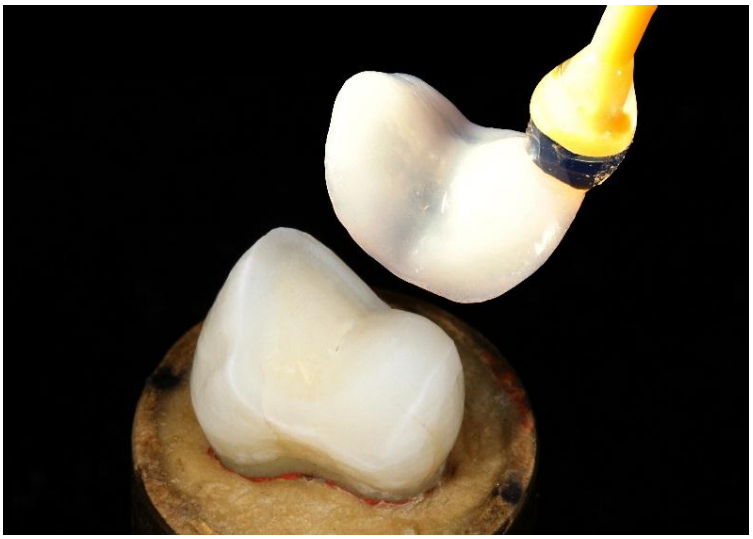

Fig. 12. Finished occlusal veneer restoration and its corresponding abutment tooth

3.5. Adhesive luting of restorations

The occlusal veneers were cleaned with 99% isopropanol in an ultrasonic cleaner for 3 min, while the teeth surface to be bonded was cleaned with fluoride-free pumice for 15 sec and rinsed thoroughly with water spray for 15 sec.

A 5% hydrofluoric acid etching gel (IPS Ceramic Etching Gel; Ivoclar Vivadent AG) was used to etch the intaglio surfaces of the occlusal veneers of groups LD and LS for 20 sec and that of group PI for 60 sec. The treated surfaces were spray-cleaned for 60 sec with distilled water and then dried with oil-free compressed air. A silane-coupling agent (Monobond Plus; Ivoclar Vivadent AG) was applied immediately to the intaglio surface of each occlusal veneer, left to react for 60 sec, and then dispersed with a stream of air, after that any remaining excess primer was dispersed with a stream of air (Fig. 13).

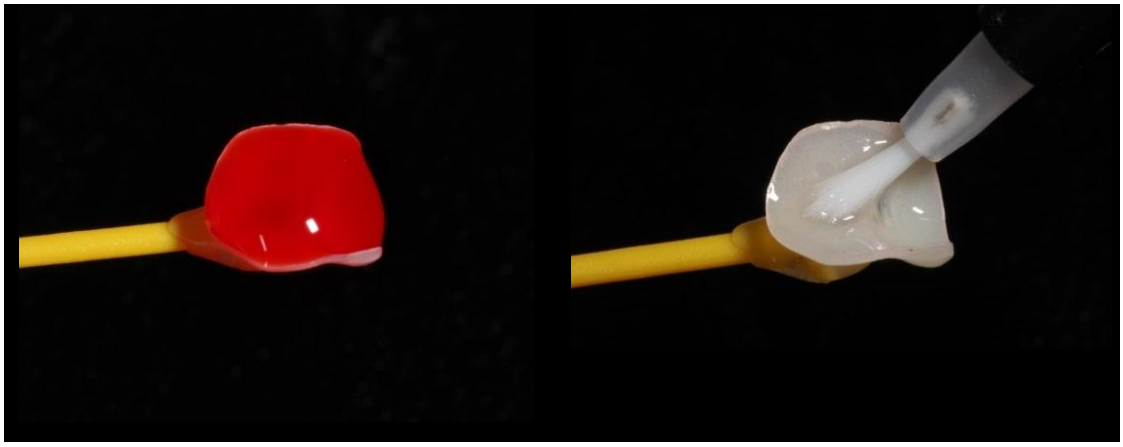

Fig. 13. Treatment of glass-ceramic restoration with 5% hydrofluoric acid etching gel and then with Monobond Plus

For the PMMA material, the intaglio surfaces of group PM were airborne-particle abraded with 50 μm Al_2O_3 at a pressure of 0.05 MPa (Fig. 14), and then cleaned for 3 min in a 99% isopropanol ultrasonic bath. Subsequently, a PMMA primer (Luxatemp-Glaze & Bond; DMG, Hamburg, Germany) was applied, and then exposed to curing light for 20 sec using a light-curing unit (Elipar 2500; 3M ESPE).

Fig. 14. Airborne-particle abrasion for group PM

The prepared teeth for each CAD/CAM material (n=32/group) were treated either with the self-etch or the etch-and-rinse bonding technique (n=16/subgroup). In the first subgroup (n=16) the prepared teeth were treated with a self-etching primer (Multilink Primer A/B; Ivoclar Vivadent AG), which was mixed in a ratio of 1:1 for 10 sec and applied for 30 sec to the prepared enamel surface with a microbrush. After that, a gentle stream of air was applied to the primed surface to evaporate volatiles, leaving the surface appearing glossy. In the second subgroup (n=16/subgroup), the prepared teeth were etched with 37% phosphoric acid (Total Etch; Ivoclar Vivadent AG) for 30 sec, the etchant was rinsed off thoroughly with water spray for 20 sec, and the teeth were dried with oil-free air. Immediately afterwards, they were conditioned with a tooth primer (Multilink Primer A/B; Ivoclar Vivadent AG) as described previously. Next, all restorations were luted adhesively to their respective prepared teeth with dual-polymerizing composite luting resin (Multilink Automix; Ivoclar Vivadent AG). The restorations were placed in position using gentle finger pressure and then loaded with a customized loading apparatus with 9.8 N (1 kg weight). The excess luting resin at the margins was removed with sponge pellets, and an air-inhibiting gel (Liquid Strip; Ivoclar Vivadent AG) was applied along the margin of the luted occlusal veneers to prevent the formation of an oxygen inhibited unpolymerized resin layer (Fig. 15). The luting material was cured using a light-curing unit (Elipar 2500; 3M ESPE) with a peak power output of 450 mW/cm^2 at a distance of 5 mm from the mesial, distal, buccal, and lingual directions for 20 sec each. After bonding, the specimens were stored in a water bath at 37°C for 3 days (Fig. 16). Finally, the specimens in every subgroup (n=16/subgroup) were assigned randomly into further subgroups (8 specimens each) either going directly to the

compressive load test or going to thermomechanical loading, and then the survived specimens underwent the compressive load test.

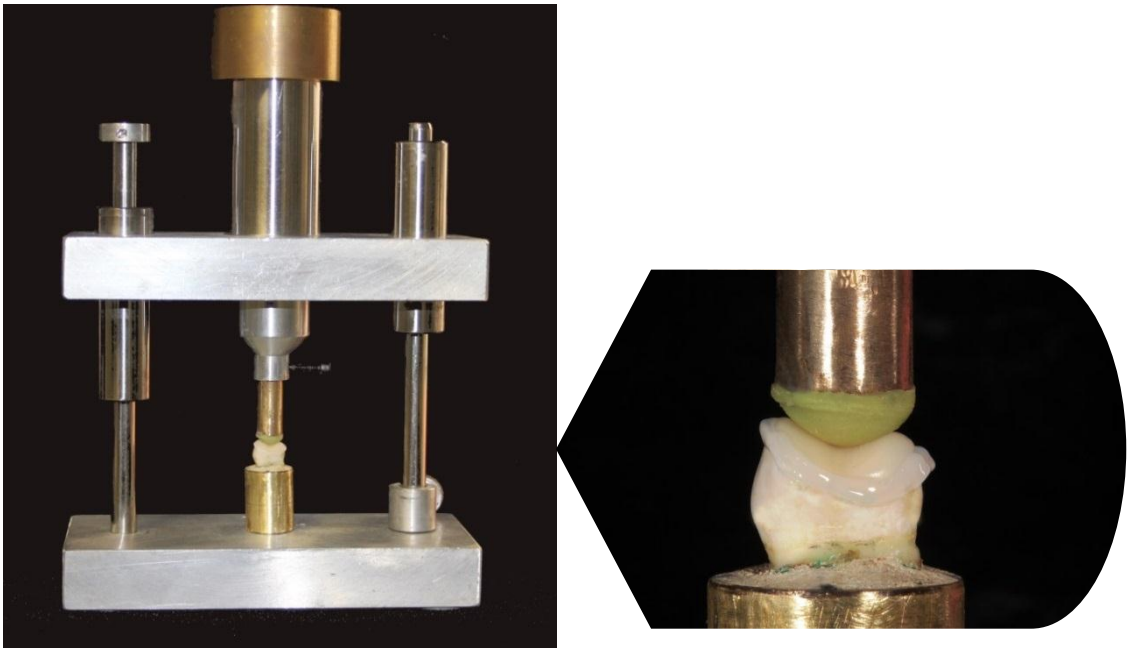

Fig. 15. Occlusal veneer luted with a load of 9.8 N

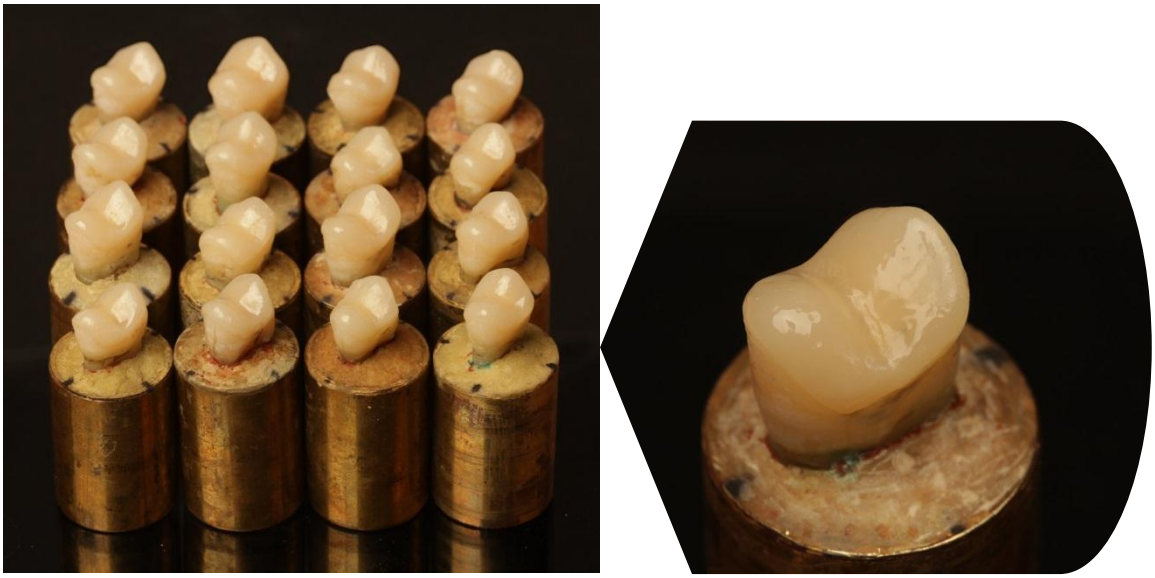

Fig. 16. Specimens after adhesive luting in group LD

3.6. Cyclic fatigue loading

To mimic the intraoral conditions and 5 years of clinical service [27,48,93], half the specimens in each subgroup (n=8) were thermomechanically fatigued in a dual-axis computerized chewing simulator (Willytec, Feldkirchen-Westerham, Germany). They were subjected to 1.2 million mechanical chewing cycles with simultaneous thermocycling between 5 and 55°C in distilled water with a 30 sec dwell time at each temperature with a total of 5,500 thermal cycles at a loading cycle frequency of 2.4 Hz. Steatite ceramic balls with a 6 mm diameter (Hoechst Ceram Tec, Wunsiedel, Germany) were used as antagonists to simulate the opposing teeth. A vertical load of 98 N (10 Kg) was applied with a vertical movement of 6 mm and a descending speed of 30 mm/sec on the buccal cusp beginning 0.5 mm below the cusp tip with a lateral sliding component of 0.3 mm towards the central fissure (Fig. 17). The test parameters of the chewing simulator are listed in Table 3. A total of 4,524 thermal cycles were performed during the course of 1.2 million cyclic fatigue. To complete 5,500 thermal cycles, additional 976 thermal cycles were conducted in a thermocycling machine (Haake W15; Willitec thermocycler, Munich, Germany). During the thermomechanical fatigue test, the specimens were monitored by means of surveillance cameras to record any failures in the specimens and to determine the number of cycles during which any failure occurred. Specimen failure was recorded for the occlusal veneers that fractured and separated from the teeth during the fatigue test.

After the thermomechanical loading was complete, all surviving specimens were inspected under a light-emitting diode (LED) light source and an optical microscope (Wild M420; Wild Heerbrugg, Gais, Switzerland) with ×5.8 magnification to detect any damage or microcracks in the restoration or tooth. Consequently, specimens were rated as completely successful when they did not show any macroscopic damage, and as partially successful when they showed some cracks without affecting the integrity of the occlusal veneer or bonding to the teeth (Fig. 18). They were rated as failure when a fracture or/and debonding occurred in the restoration.

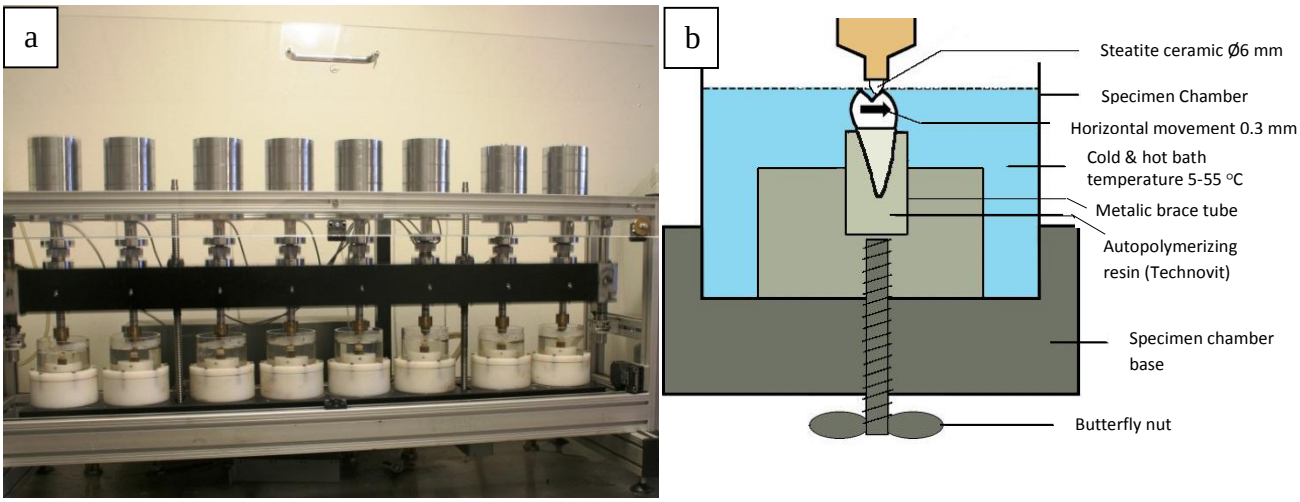

Fig. 17. a. Multifunction chewing simulator (Willytec), b. Schematic diagram of one specimen chamber

Table 3. Test parameters of the chewing simulator

Cold/hot bath temperature	5°C/55°C
Vertical movement	6 mm
Rising speed	55 mm/sec
Descending speed	30 mm/sec
Weight per specimen	98 N (10 Kg)
Kinetic energy	2,250 x 10-6 J
Dwell time	30 sec
Horizontal movement	0.3 mm
Forward speed	30 mm/sec
Backward speed	55 mm/sec
Cycle frequency	2.4 Hz

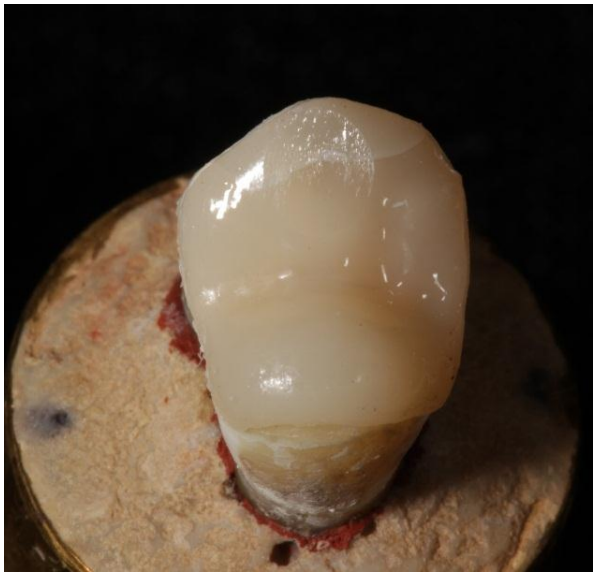

Fig. 18. Specimen showing some cracks after thermomechanical loading (partial success)

3.7. Quasi-static loading test

All non-aged and survived (complete and partial success) aged specimens were statically loaded until failure. To determine the specimens' fracture strength, a stainless steel bar with a 6 mm-diameter ball-end mounted in a universal testing machine (Zwick Z010/TN2A; Zwick, Ulm, Germany) was used to apply a quasi-static load, which was centered at the fissure along the long axis of the restored tooth at a cross-head speed of 1 mm/min until failure. Additionally, a 0.5 mm tin foil was placed between the specimens and the stainless steel bar to avoid local stress concentration (Fig. 19). The fracture loads were recorded automatically in Newtons (N) for each specimen by means of the testing software (testXpert II V 3.3, Zwick/Roell). Specimens were considered as having failed the static fracture strength test when the stress strain curve dropped by 10%. This threshold was important especially for group PM because of the plastic deformation of the PMMA material.

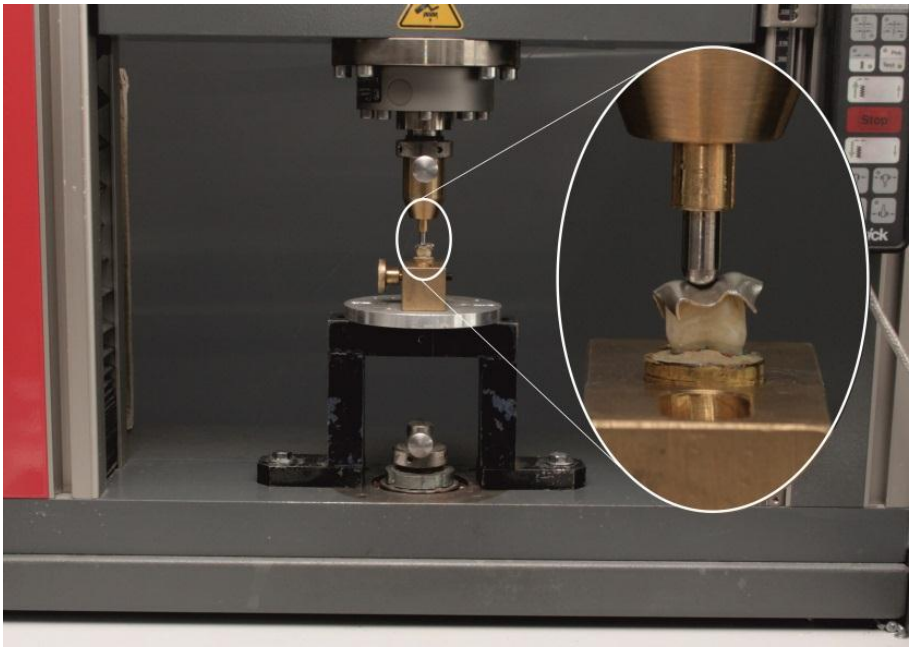

Fig. 19. Universal testing machine (Zwick Z010/TN2A)

3.8. Mode of failure

After the fracture strength test, all specimens were inspected under an LED light source and an optical microscope (Wild M420; Wild Heerbrugg) with ×20 magnifications to evaluate the mode of failure. The failure mode was classified into 4 categories in accordance with Guess et al. [39] class I: extensive crack formation within the restoration, class II: cohesive failure within the restoration, class III: debonding failure between the restoration and tooth structures, and class IV: longitudinal failure of the restoration and tooth involving root.

3.9. Statistical analysis

Normal distribution of the data was explored using the Shapiro-Wilk test, which revealed that the data were not normally distributed. As a result, the Kruskal-Wallis test and Mann-Whitney U tests were used for statistical analysis. The Kruskal-Wallis test was used first to detect the overall significance, while the Mann-Whitney U tests were used to identify which pairs of groups demonstrated a significant difference (α=0.05). Statistical analysis was performed with statistical software (IBM SPSS Statistics v20.0; IBM Corp).

4. RESULTS

The cumulative survival rate after the thermomechanical fatigue of the four self-etch groups were as the following: group LD-SE 50%, group LS-SE 62.5%, group PI-SE 37.5%, and group PM-SE 50%. Although the surviving specimens may have exhibited some microcracks, the integrity of the specimens or bonding to the teeth was not affected. The results regarding the cumulative survival rate as well as the descriptive complete and partial success for the studied groups are shown Table 4. In contrast, all specimens in the etch-and-rinse groups survived the thermomechanical loading without any kind of damage (complete success).

Table 4. Percentage of surviving specimens after thermomechanical fatigue

Group	Self-etching			Etch-and-rinse
	Complete success	Partial success	Cumulative survival rate after 1.2 million cycles	Complete success
Lithium disilicate (LD)	50%	0%	50%	100%
Zirconia-reinforced lithium silicate (LS)	25%	37.5%	62.5%	100%
Polymer-infiltrated ceramic (PI)	0%	37.5%	37.5%	100%
Polymethylmethacrylate PMMA (PM)	50%	0%	50%	100%

The failed specimens of the self-etching groups in the fatigue test fractured under a load of 98 N. Therefore, their fracture strength was reported as 98 N rather than 0 N (98 N was the applied vertical load during the dynamic loading). Accordingly, the minimum fracture strength of self-etching groups after thermomechanical fatigue was 98 N, while the maximum fracture strength was 1,250 N in group LS-SE. The results of the quasi-static load to fracture test of the groups are listed in Table 5, and the failure mode's descriptive statistics are presented in Fig. 20. After quasi-static loading to failure, the most commonly observed failure modes were extensive crack formation within the restoration (class I) and debonding failure between the restoration and tooth structures (Class III) for all the groups (Fig. 21).

Table 5. Fracture strength of groups in Newton [N], means, standard deviations (SD), medians, lower and upper quartiles, minima and maxima (n=8). Medians of different etching/bonding techniques within the same material with the same upper case superscript letters within the same column are not statistically different (p>0.05). Medians of different materials within the same etching/bonding technique with the same lower case subscript letters within the same column are not statistically different (p>0.05). Medians with the same Greek letters within the same raw are not statistically different (p>0.05). Group codes see Table 1.

	Without thermomechanical loading				After thermomechanical loading			
Group Codes	**Median**	**Q1 Q3**	**Min Max**	**Mean ±SD**	**Median**	**Q1 Q3**	**Min Max**	**Mean ±SD**
LD-SE	**782.5** $^{B}_{ab}$ α	686.5 849.5	586 1,210	806.1 ±186.9	**328.5** $^{B}_{a}$ α	98 941.3	98 1,070	470.8 ±428.2
LD-E&R	**1,335** $^{A}_{a}$ α	1,220 1,635	1,150 1,730	1,408.8 ±215.8	**1,560** $^{A}_{a}$ α	1,372.5 1,700	1,300 1,770	1,545 ±175.2
LS-SE	**668.5** $^{B}_{b}$ α	615 727.8	579 869	684 ±90	**881.5** $^{B}_{a}$ α	98 1,010.8	98 1,250	663.8 ±482.7
LS-E&R	**1,015** $^{A}_{b}$ α	839.5 1,285	616 1,670	1,076.8 ±324.9	**1,735** $^{A}_{a}$ β	1,495 1,842.5	1,360 1,860	1,667.5 ±189.1
PI-SE	**769.5** $^{B}_{ab}$ α	670 867	565 975	767.1 ±130.9	**98** $^{B}_{a}$ β	98 738	98 861	349.9 ±350.5
PI-E&R	**1,005** $^{A}_{b}$ α	863.5 1,185	798 1,190	1,018.5 ±155.5	**1,310** $^{A}_{b}$ β	1,162.5 1,567.5	848 1,680	1,321 ±269.1
PM-SE	**909.5** $^{A}_{a}$ α	750.3 1,027.5	634 1,120	897.5 ±164	**434** $^{B}_{a}$ β	98 839	98 888	462 ±390.8
PM-E&R	**994** $^{A}_{b}$ α	845.5 1,112.8	593 1,290	974.5 ±208.4	**1,130** $^{A}_{b}$ β	1,032.5 1,497.5	1,010 1,530	1,232.5 ±223.1

The statistical analysis revealed that the etch-and-rinse bonding technique increased significantly the median fracture strength of the CAD/CAM restorative materials (P≤0.05) in comparison to the self-etch bonding technique regardless of fatigue loading protocol, with the exception of group PM, where the etch-and-rinse bonding technique without thermomechanical loading had no statistically significant influence (P>0.05). Thermomechanical fatigue loading increased the fracture strength of groups LS, PI, and PM when the etch-and-rinse bonding technique was used (P≤0.05), whereas it did not affect group LD (P>0.05). In contrast, thermomechanical loading reduced the fracture strength of groups PI and PM significantly when bonded with the self-etch bonding technique (P≤0.05).

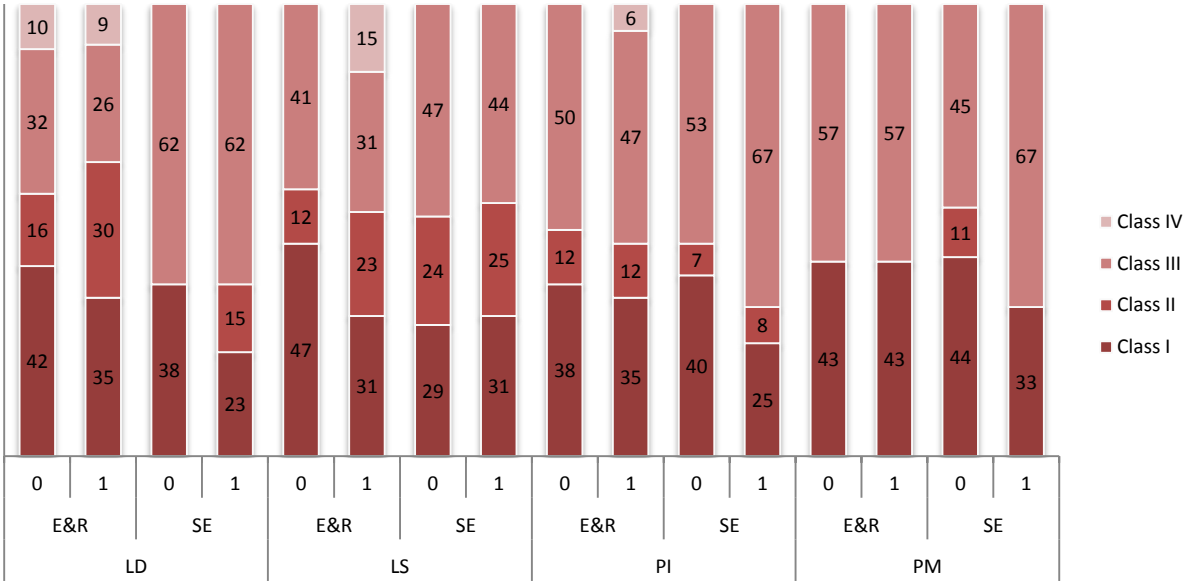

Fig. 20. Percentage (%) of failure mode. I: Extensive crack formation within restoration. II: Cohesive failure within restoration. III: Debonding failure between restoration and tooth structures. IV: Longitudinal failure of restoration and tooth involving root

Considering the type of CAD/CAM material, a significant difference of fracture strength was revealed when etch-and-rinse etching technique was used, so that without thermomechanical loading, group LD showed a significantly higher fracture strength than the other groups ($P \leq 0.05$). However, after thermodynamic loading, groups LD and LS showed significantly higher fracture strengths than groups PI and PM ($P \leq 0.05$). However, when the CAD/CAM materials were bonded with the self-etch bonding technique, without thermomechanical loading only the median fracture strength of groups LS and PM differed significantly ($P=0.015$).

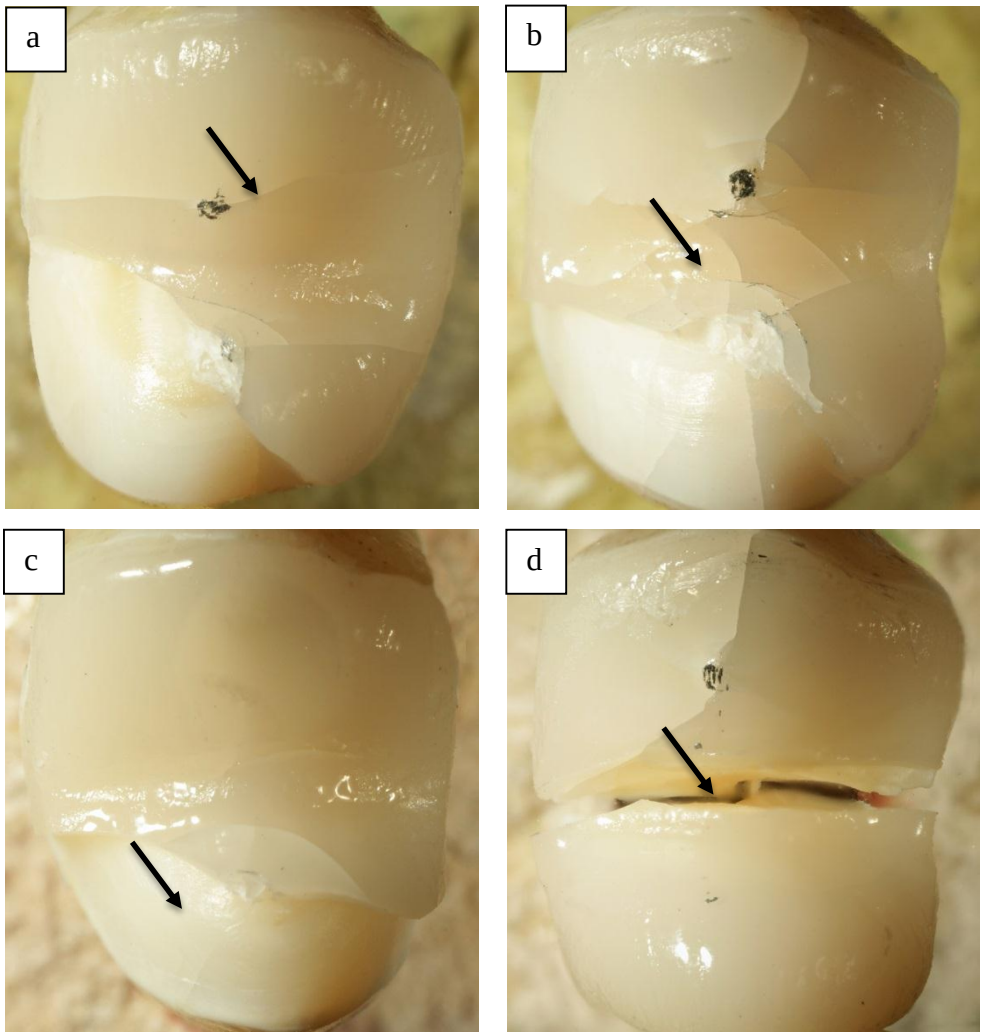

Fig. 21. Exemplary modes of failure denoted with arrow: a. (I), b. (II), c. (III), d. (IV).
Definition see page 29

Regarding the influence of the used etching protocol, without thermomechanical loading, the etch-and-rinse-technique had significantly higher fracture strengths within the same CAD/CAM material of groups LD, LS, and PI in comparison to the self-etch bonding technique. The median fracture strengths for the four groups were as follows: lithium disilicate was 1,335 N in group LD-E&R and 782.5 N in group LD-SE (P=0.001), zirconia-reinforced lithium silicate was 1,015 N in group LS-E&R and 668.5 N in group LS-SE (P=0.007), and polymer-infiltrated ceramic was 1,005 N in group PI-E&R 769.5 N in group PI-SE (P=0.007). In contrast, the PMMA material showed no significant difference between group PM-E&R (994 N) and group PM-SE (909.5 N; P>0.05).

After thermomechanical loading, the etch-and-rinse-technique resulted in significantly higher fracture strengths within the same CAD/CAM material of the four tested groups (P=0.001) in comparison to the self-etch bonding technique. The median fracture strengths were as follows: lithium disilicate was 1,560 N in group LD-E&R and 328.5 N in group LD-SE, zirconia-reinforced lithium silicate was 1,735 N in group LS-E&R and 881.5 N in group LS-SE, polymer-infiltrated ceramic increased was 1,310 N in group PI-E&E and 98 N in group PI-SE, and PMMA was 1,130 N in group PM-E&R and 434 N in group PM-SE.

Regarding the influence of thermomechanical loading, in the groups bonded with the self-etch bonding technique, thermomechanical loading decreased significantly the median fracture strength of group PI from 769.5 N to 98 N (P=0.047) and group PM from 909.5 N to 434 N (P=0.025). However, thermomechanical loading did not significantly influence the median fracture strength of groups LD (P>0.05) and LS (P>0.05). On the contrary, the groups bonded with the etch-and-rinse bonding technique, thermomechanical loading increased significantly the median fracture load of group LS from 1,015 N to 1,735 (P=0.001), group PI from 1,005 N to 1,310 N (P=0.030), and group PM from 994 N to 1,130 N (P=0.037), the median fracture strength of group LD also increased from 1,335 N to 1,560 N but this was not statistically significant (P>0.05).

5. DISCUSSION

To ensure a close simulation of the clinical situations, all procedures in the recent study were designed to simulate valid applied clinical protocols. Of course, clinical trials remain the ideal strategy in scientific experiments in the field of adhesive dentistry. But for ethical reasons, preclinical laboratory tests are pre-requirements before clinical trials. However, many variables in the oral environment may affect and covariate the interested one, and therefore might influence the actual results [72]. Therefore, laboratory investigations including thermocycling and dynamic loading are of great importance to test new dental materials with accelerated conditions mimicking the actual intraoral conditions [27,48,93].

5.1. Discussion of methodology

Several factors influence the fracture strength of ceramic restorations, such as kind of restorative material [22], thickness of restoration [82], preparation design [39], tooth adherend substrates [22], adhesive system [25], and loading mode [63]. Natural human teeth were used in this study to achieve a high clinical relevance. The antimicrobial storage media 0.1 % thymol was used since the collected teeth had to be stored for an extended period as the collection proceeded [81]. Moreover, physiological tooth mobility was simulated through the application of 0.2 mm thick gum resin on the roots of the teeth to imitate the periodontal membrane, which is important for the absorption and distribution of stresses generated by masticatory forces over teeth into the alveolar bone [75]. Hence, different elastomeric materials [89] have been used in various laboratory studies to simulate the natural periodontal ligaments [7,22,39,76].

The sample size of this study was justified to follow previous studies, which were carried out by our group with the same study design and sources of variations, and these studies' sample sizes gave acceptable standard deviations and allowed the statistical differentiation of the evaluated factors. In addition, the chewing simulator machine accepts only 8 specimens per test making this an ideal manageable group size [6,7,22,82,97].

Tooth morphology and preparation geometry have been shown to influence the longevity and the reliability of prosthetic restorations [86]. Therefore, premolars used in this current study were selected to be as similar as possible in dimensions, i.e. mesiodistally and buccolingually. Also, the preparation design was chosen based on the general guidelines recommended for minimally invasive partial coverage ceramic restorations [1,49]. To standardize the preparation geometry, the cusp inclinations were designed to have a 120-degree angle with rounded angles [76,90]. The

parameters used for masticatory simulation were adjusted to the reported physiological values [48,93].

The reduced thickness of the occlusal veneers in this study compared to the manufacturers' recommendations was carried out to evaluate a minimally invasive preparation of dental hard tissues. Moreover, minimally invasive restorations provide a better bond strength when adhesively bonded to enamel than when bonded to dentin [72]. Besides, thin occlusal veneer restorations revealed a comparable fracture strength to that of thick occlusal veneers when adhesively bonded to natural teeth [22,39,54].

Limitations of the current study that may affect the clinical interpretation of the results, include the difficulty in performing an equal amount of enamel layer preparation, the lack of evaluation of wear of the occlusal veneers after the thermomechanical loading, the use of different loading points during dynamic and static loading, the limited number of specimens tested, the use of water rather than artificial saliva during testing, and the difficulty in replicating exact clinical conditions.

5.2. Discussion of results

5.2.1. Influence of the CAD/CAM restorative materials

The fracture strength of the four tested dental CAD/CAM materials in this study did not correspond to their respective uniaxial flexural strength (according to the manufacturers' scientific documentations) of 530, 420, 160, and 130 MPa for lithium disilicate, zirconia-reinforced lithium silicate, polymer-infiltrated ceramic, and PMMA, respectively. This confirmed that the mechanical behavior of the restored tooth complex, that is the restorative material, adhesive system, and restored tooth cannot be easily predicted [45,62]. Furthermore, strong adhesive bonding with luting resin can noticeably strengthen weaker ceramic restorations and balance the inherent strength variations among different materials [13].

The first part of the null hypothesis that the different tested CAD/CAM materials would not influence the fracture strength of the tested occlusal veneers was partially rejected. After thermomechanical loading, occlusal veneers made from zirconia-reinforced lithium silicate (group LS-E&R) and lithium disilicate (group LD-E&R) showed significantly higher fracture strengths than occlusal veneers made from the resin-containing materials (groups PI-E&R and PM-E&R; $P \leq 0.05$). Likewise, without thermomechanical loading, lithium disilicate occlusal veneers (group LD-E&R) demonstrated significantly higher fracture strength than the other

groups (LS-E&R, PI-E&R, and PM-E&R) when bonded with the etch-and-rinse bonding technique ($P \leq 0.05$). These results are in agreement with the findings of Kois et al. [54] as they reported a significant higher fracture strength of lithium disilicate partial coverage restorations in comparison to other glass-ceramic materials. The reason for these results might be the differing mechanical properties of the tested restorative CAD/CAM materials [9,13,34]. This could be also related to the monolithic structural property of lithium disilicate ceramic, which facilitates a proper etching pattern using hydrofluoric acid. This suggests that the bond strength dominates over the differences between the materials [17].

The mode of failure in thin (less than 1 mm) monolithic ceramic restorations is initiating from the luting surface with subsequent upward propagation, leading to bulk fracture of restoration [99]. However, the difference of modulus of elasticity between restorative material, luting materials, and tooth adherent surface determine the character of the radial fracture [57]. This observation was noticed in the current study, as the extensive crack formation within the restoration (class I) and the debonding failure between the restoration and tooth (class III) were prevalent in all groups. Whereas, the longitudinal restoration and tooth failure involving root (class IV) was only recorded in the glass-ceramic groups when they were bonded with the etch-and-rinse bonding technique to the teeth.

5.2.2. Influence of the bonding technique

The present study showed that the final median fracture strengths of groups bonded with the etch-and-rinse bonding technique were higher than those reported for natural unrestored human maxillary premolars (958 N) [5]. Moreover, they were higher than the maximum parafunctional masticatory forces (up to 1,000 N) [37].

The second part of the null hypothesis that the different bonding techniques would not influence the fracture strength of the tested occlusal veneers had to be almost completely rejected. After thermomechanical loading, the etch-and-rinse bonding technique showed a statistically significant increase of the fracture strength for all test groups ($P=0.001$). Even without thermomechanical loading, the etch-and-rinse bonding technique showed also a highly statistically significant increase in the fracture strength of groups LD, LS, and PI ($P \leq 0.05$). Only group PM recorded a non-significant difference between the etch-and-rinse and self-etching bonding technique ($P>0.05$). The increase in fracture strength can be attributed to the obtained porous enamel surface morphology after the application of the 37% phosphoric acid etchant in

the etch-and-rinse groups, resulting in a higher fracture strength due to a higher adhesion at the interface between the adhesive luting resin and the enamel. The proper morphological etch pattern and the positive adhesion effect after using phosphoric acid on enamel has been observed in different previous studies [35,87,95].

In this current study, with comparison to the self-etching groups, the etch-and-rinse groups recorded not only noticeable higher fracture strengths but also thermomechanical fatigue increased significantly the fracture strengths of these groups. The higher survival rates and fracture strengths in the aforementioned studies [22,82,98] might be explained by the use of etch-and-rinse bonding technique on enamel, which clearly played a major role in determining the survival ability of the test specimens. In addition to the use of molars with a wider preparation angles, higher ceramic thickness [22,98], and fewer masticatory cycles [22,82] may be additional reasons for the high survival rates and high fracture strength reported in the previous studies. In contrast, the lower median fracture strengths in a study of Guess et al. [39] in comparison to the recorded fracture strength of group LD-E&R in the current study with 1,560 N might be due to the extension of the occlusal onlays to restore the occlusal and the proximal walls of the premolars or/and due to the lower vertical load which was applied during the thermomechanical fatigue. Guess et al. emphasized that occlusal veneers with a 0.5 mm thickness bonded to enamel had a fracture strength comparable with that of 2 mm thick occlusal veneers bonded to dentin [39].

The improved fracture strength of ultrathin occlusal onlays is due to superior bonding to enamel as compared to bonding to dentin. Weak and/or thin restorations are noticeably strengthened when luted with a strong adhesive bonding system. Therefore when firmly bonded to enamel, these weak and/or thin restorations behave in a manner similar to strong and/or thick restorations [13,39]. On the contrary, a study of Yazigi et al. [97] compared the efficiency of immediate dentin sealing and the effects of different bonding protocols on the fracture strength of lithium disilicate CAD/CAM occlusal veneers. Even though the preparation and adhesive bonding were limited to dentin with margins in enamel, the recorded mean of fracture strength values ranged from 1,122 N to 1,853 N, which make it comparable to the values recorded in the etch-and-rinse groups (LD-E&R and LS-E&R) in the current study despite dentin being a supposedly inferior substrate for adhesive bonding. These findings might be attributed to the proper selection of bonding technique to dentin as well a precise design of occlusal veneers in the both studies.

5.2.3. Influence of the thermomechanical fatigue

The third part of the null hypothesis that thermomechanical loading would not influence the fracture strength of the tested occlusal veneers was partially rejected. Thermomechanical loading significantly increased the fracture strength of groups LS, PI, and PM ($P \leq 0.05$) when bonded with the etch-and-rinse bonding technique. This increase might be explained by the strong bond achieved by the etch-and-rinse bonding technique between the restoration and the enamel occlusal surface [35]. Whereas, thermomechanical fatigue significantly reduced the fracture strength of group PI and group PM ($P \leq 0.05$) when bonded with the self-etching bonding technique. The change of temperature between 5 and 55 °C for 5,500 cycles during the process of thermomechanical fatigue might lead to thermal expansion and shrinkage of the polymer contents of these two resin containing groups. This might have accelerated their fatigue during the thermomechanical loading procedure, resulting in a statistically significant decrease in their final fracture strength [32]. However, failed specimens during the thermomechanical fatigue test in groups PI and PM were able to survive more chewing cycles in comparison to groups LD and LS. These findings are consistent with two previous laboratory studies, which showed that thin occlusal veneers made from CAD/CAM composite resin materials had a significantly higher stepwise loading fatigue resistance when compared with lithium disilicate material [63,84]. As neither study [63,84] used thermocycling during the fatigue dynamic loading procedures and followed a stepwise loading fatigue from 200 N up to 1,400 N at a maximum of 185,000 cycles without testing the specimens under static load, any comparison with the present study is limited.

All specimens in etch-and-rinse groups survived the thermomechanical fatigue loading. However, nearly half of the specimens in the self-etching groups failed during the thermomechanical fatigue as shown in Table 4. A laboratory study [82] reported that occlusal veneers luted to enamel with self-etching bonding technique had a survival rate after 600,000 thermodynamic loading cycles of 75%. However, some previous studies [22,39] reported that all occlusal veneer restorations luted to enamel with etch-and-rinse bonding technique survived the whole applied thermomechanical loading cycles. The lower ability of self-etching primer to etch enamel than etching with phosphoric acid was observed in previous studies [35,87,95]. Therefore, our findings are in agreement with the former studies.

6. CONCLUSIONS

Based on the findings of this laboratory study, the following conclusions can be drawn:

1. Considering the survivability and the fracture strength of the occlusal veneers, all tested CAD/CAM materials may be considered as a viable treatment for restoring the occlusal surfaces of posterior teeth when bonded to enamel with the etch-and-rinse bonding technique.
2. Thermomechanical fatigue loading generally decreased the survival rate and final fracture strength of the all tested CAD/CAM materials when bonded to enamel using a self-etching bonding technique as compared to the etch-and-rinse bonding technique.
3. The self-etching bonding technique cannot be recommended for luting thin minimally invasive occlusal veneers to enamel, as their long-term survivability is questionable.

7. SUMMARY

Various new CAD/CAM restorative dental materials have been developed for indirect restorations with the assumption of better physical and mechanical properties than the well-known classical materials. Therefore, this study was designed to evaluate the influence of adhesive luting technique and thermomechanical fatigue loading on the durability and fracture strength of minimally invasive occlusal veneer restorations fabricated from four CAD/CAM materials.

The occlusal surfaces of 128 extracted human maxillary premolars were prepared within the enamel layer and restored with occlusal veneers with a fissure/cusp thicknesses of 0.5/0.8 mm made from the different dental CAD/CAM materials (n=32/group): group LD: lithium disilicate (e.max CAD), group LS: zirconia-reinforced lithium silicate (Vita Suprinity), group PI: polymer-infiltrated ceramic (Vita Enamic), and group PM: polymethylmethacrylate (PMMA, Telio CAD). The prepared teeth were either conditioned by a self-etching primer (Multilink Primer A/B, groups SE) or pre-etched with phosphoric acid prior to the primer application (Total etch, groups E&R) (n=16/subgroup). The occlusal veneers were then bonded using an adhesive luting system (Multilink Automix). To simulate a clinical service of 5 years, half of the specimens (n=8) in each subgroup were subjected to thermomechanical fatigue loading between 5-55 °C in a chewing simulator (1.2 million cycles at 98 N and with 5,500 thermal cycles). Finally, all specimens were quasi-statically loaded until failure. The statistical analysis was made using Kruskal-Wallis test and Mann-Whitney U tests (α=0.05).

All specimens in the etch-and-rinse groups LD-E&R, LS-E&R, PI-E&R, and PM-E&R survived the thermomechanical loading without damage. Whereas some specimens in self-etch groups LD-SE, LS-SE, PI-SE, and PM-SE did not withstand the thermomechanical fatigue loading and the survival rates ranged from 37.5% in group PI-SE to 62.5% in group LS-SE.

The median fracture strengths in Newton (N) of self-etching groups were: Without thermomechanical loading, LD-SE: 782.5, LS-SE: 668.5, PI-SE: 769.5, and PM-SE: 909.5, and after thermomechanical loading, LD-SE: 328.5, LS-SE: 881.5, PI-SE: 98, and PM-SE: 434. Etch-and-rinse groups recorded the following median fracture strengths: Without thermomechanical loading, LD-E&R: 1,335, LS-E&R: 1,015, PI-E&R: 1,005, and PM-E&R: 994, and after thermomechanical loading, LD-E&R: 1,560, LS-E&R: 1,735, PI-E&R: 1,310, and PM-E&R: 1,130.

Statistical analysis revealed that in comparison to the self-etching luting technique, the etch-and-rinse luting technique increased significantly the median fracture strengths of the CAD/CAM restorative materials ($P \leq 0.05$) regardless of the loading protocol, with the exception of group PM without thermomechanical loading where the bonding technique had no statistically significant influence ($P > 0.05$). Moreover, thermomechanical loading improved the fracture strength of groups LS, PI, and PM when the etch-and-rinse bonding technique was used ($P \leq 0.05$), whereas it did not influence group LD ($P > 0.05$). In contrast, thermomechanical loading reduced the fracture strengths of groups PI and PM significantly when bonded with the self-etch bonding technique ($P \leq 0.05$).

The comparison between the four CAD/CAM materials revealed that, without thermomechanical loading, group PM-SE showed significantly higher fracture strength than group LS-SE ($P = 0.015$), as well as group LD-E&R showed a significantly higher fracture strength than groups LS-E&R, PI-E&R, and PM-E&R ($P \leq 0.05$). However, after thermomechanical loading, groups LD-E&R and LS-E&R showed significantly higher fracture strengths than groups PI-E&R and PM-E&R ($P \leq 0.05$).

As a conclusion, when the four tested CAD/CAM occlusal veneer restorations are luted to enamel, the etch-and-rinse etching technique improved the overall stability, reliability, longevity, and fracture strength of the four tested CAD/CAM occlusal veneer restorations as compared to the self-etching technique, which cannot be recommended for occlusal veneers bonded to enamel.

8. ZUSAMMENFASSUNG

Verschiedene neue restaurative CAD/CAM-Dentalmaterialien wurden für indirekte Restaurationen entwickelt. Sie sollen bessere physikalische und mechanische Eigenschaften als die bekannten klassischen Materialien aufweisen. Das Ziel dieser vorliegenden Studie war, den Einfluss künstlicher Alterung sowie der Klebetechniken auf die Haltbarkeit und Bruchfestigkeit von minimal-invasiven okklusalen Veneers, die aus vier CAD/CAM-Materialien hergestellt wurden, zu evaluieren.

Es wurden 128 Kauflächen von extrahierten menschlichen oberen Prämolaren innerhalb des Schmelzes präpariert und mit okklusalen Veneers mit einer Fissur/Höcker-Dicke von 0,5/0,8 mm aus den verschiedenen zahnärztlichen CAD/CAM-Materialien hergestellt (n=32/Gruppe): Gruppe LD: Lithiumdisilikatkeramik (e.max CAD), Gruppe LS: zirkondioxidverstärkte Lithiumsilikatkeramik (Vita Suprinity), Gruppe PI: Polymer-infiltrierte Keramik (Vita Enamic) und Gruppe PM: Polymethylmethacrylat (PMMA, Telio CAD). Die präparierten Zähne wurden in jeder Gruppe entweder mit selbstätzendem Primer (Multilink Primer A und B, Gruppen SE) ohne separate Ätzung oder mittels separater Phosphorsäureätzung (Etch-and-rinse, Gruppen E&R) (n=16/Untergruppe) vorbehandelt. Die Restaurationen wurden dann mit Kompositkunststoff (Multilink Automix) adhäsiv befestigt. Um eine klinische Belastung von 5 Jahren zu simulieren, wurde die Hälfte jeder Untergruppe (n=8) in einem Kausimulator 1,2 Million Zyklen mit 98 N dynamischer Belastung und 5.500 thermischen Zyklen von 5-55 °C ausgesetzt. Anschließend wurden alle Proben durch Druckbelastung bis zum Versagen belastet. Die statistische Analyse wurde mit den Tests von Kruskal-Wallis und Mann-Whitney-U (α=0,05) durchgeführt.

Alle Proben aus der Etch-and-Rinse-Gruppen LD-E&R, LS-E&R, PI-E&R und PM-E&R überlebten die thermomechanische Belastung ohne Schaden. Die Selbstätzgruppen LD-SE, LS-SE, PI-SE und PM-SE hingegen wiesen lediglich Überlebensraten von 37,5% in der Gruppe PI-SE bis max. 62,5% in der Gruppe LS-SE auf.

Die Medianwerte der Bruchfestigkeit (in Newton) waren für die Selbstätzgruppen: vor der künstlichen Alterung, LD-SE: 782,5, LS-SE: 668,5, PI-SE: 769,5, und PM-SE: 909,5, und nach der künstlichen Alterung, LD-SE: 328,5, LS-SE: 881,5, PI-SE: 98, und PM-SE: 434. Die Etch-and-Rinse-Gruppen erreichten die folgenden medianen Bruchfestigkeiten: vor der künstlichen

Alterung, LD-E&R: 1.335, LS-E&R: 1.015, PI-E&R: 1.005, und PM-E&R: 994, und nach der künstlichen Alterung, LD-E&R: 1.560, LS-E&R: 1.735, PI-E&R: 1.310, und PM-E&R: 1.130.

Die statistische Analyse ergab, dass die medianen Bruchfestigkeiten der mit Etch-and-Rinse-Technik befestigten CAD/CAM-Materialien im Vergleich zu mit Selbstätztechnik befestigten Materialien unabhängig vom Belastungsprotokoll deutlich erhöht waren ($P \leq 0,05$). Eine Ausnahme war nur in der Gruppe PM ohne thermomechanische Belastung zu erkennen, in der kein statistisch signifikanter Einfluss der Befestigungstechnik nachzuweisen war ($P > 0,05$). Außerdem verbesserte die thermomechanische Belastung die Bruchfestigkeit der Gruppen LS, PI und PM, wenn die Etch-and-Rinse-Technik ($P \leq 0,05$) verwendet wurde, während sie die Gruppe LD ($P > 0,05$) nicht beeinflusste. Im Gegensatz dazu reduzierte die thermomechanische Belastung die Bruchfestigkeit der Gruppen PI und PM signifikant, wenn diese mit der Selbstätztechnik ($P \leq 0,05$) befestigt wurden.

Der Vergleich zwischen den vier CAD/CAM-Materialen ergab, dass die Gruppe PM-SE ohne thermomechanische Belastung eine deutlich höhere Bruchfestigkeit als die Gruppe LS-SE ($P = 0,015$) aufwies. Die Gruppe LD-E&R zeigte eine deutlich höhere Bruchfestigkeit als die Gruppen LS-E&R, PI-E&R und PM-E&R ($P \leq 0,05$). Auf der anderen Seite zeigten die Gruppen LD-E&R und LS-E&R nach thermomechanischen Belastung deutlich höhere Bruchfestigkeiten als die Gruppen PI-E&R und PM-E&R ($P \leq 0,05$).

Aus den Ergebnissen der Studie kann man schließen, dass die vier getesteten okklusalen CAD/CAM Veneer-Restaurationen mittels Ätztechnik auf Schmelz verklebt, eine deutlich erhöhte Gesamtstabilität, Zuverlässigkeit, Langlebigkeit, sowie Bruchfestigkeit durch die Anwendung der Säureätztechnik erzielten, als wenn sie selbstätzend angewendet wurden. Daher kann die selbstätzende Technik nicht für die Befestigung okklusaler Veneers auf Schmelz empfohlen werden.

9. REFERENCES

[1] Ahlers MO, Mörig G, Blunck U, Hajto J, Probster L, Frankenberger R. Guidelines for the preparation of CAD/CAM ceramic inlays and partial crowns. Int J Comput Dent 2009;12:309-25.

[2] Albakry M, Guazzato M, Swain MV. Biaxial flexural strength, elastic moduli, and x-ray diffraction characterization of three pressable all-ceramic materials. J Prosthet Dent 2003;89:374-80.

[3] Albashaireh ZS, Ghazal M, Kern M. Two-body wear of different ceramic materials opposed to zirconia ceramic. J Prosthet Dent 2010;104:105-13.

[4] Albero A, Pascual A, Camps I, Grau-Benitez M. Comparative characterization of a novel cad-cam polymer-infiltrated-ceramic-network. J Clin Exp Dent 2015;7:495-500.

[5] Attia A, Abdelaziz KM, Freitag S, Kern M. Fracture load of composite resin and feldspathic all-ceramic CAD/CAM crowns. J Prosthet Dent 2006;95:117-23.

[6] Attia A, Kern M. Fracture strength of all-ceramic crowns luted using two bonding methods. J Prosthet Dent 2004;91:247-52.

[7] Attia A, Kern M. Influence of cyclic loading and luting agents on the fracture load of two all-ceramic crown systems. J Prosthet Dent 2004;92:551-6.

[8] Awad D, Stawarczyk B, Liebermann A, Ilie N. Translucency of esthetic dental restorative CAD/CAM materials and composite resins with respect to thickness and surface roughness. J Prosthet Dent 2015;113:534-40.

[9] Awada A, Nathanson D. Mechanical properties of resin-ceramic CAD/CAM restorative materials. J Prosthet Dent 2015;114:587-93.

[10] Bedran-Russo A, Leme-Kraus AA, Vidal CMP, Teixeira EC. An overview of dental adhesive systems and the dynamic tooth-adhesive interface. Dent Clin North Am 2017;61:713-31.

[11] Behr M, Rosentritt M, Mangelkramer M, Handel G. The influence of different cements on the fracture resistance and marginal adaptation of all-ceramic and fiber-reinforced crowns. Int J Prosthodont 2003;16:538-42.

[12] Bicalho AA, Tantbirojn D, Versluis A, Soares CJ. Effect of occlusal loading and mechanical properties of resin composite on stress generated in posterior restorations. Am J Dent 2014;27:129-33.

[13] Bindl A, Lüthy H, Mörmann WH. Strength and fracture pattern of monolithic CAD/CAM-generated posterior crowns. Dent Mater 2006;22:29-36.

[14] Blatz MB, Sadan A, Arch GH, Jr., Lang BR. In vitro evaluation of long-term bonding of Procera AllCeram alumina restorations with a modified resin luting agent. J Prosthet Dent 2003;89:381-7.

[15] Blatz MB, Sadan A, Kern M. Resin-ceramic bonding: a review of the literature. J Prosthet Dent 2003;89:268-74.

[16] Blatz MB, Sadan A, Martin J, Lang B. In vitro evaluation of shear bond strengths of resin to densely-sintered high-purity zirconium-oxide ceramic after long-term storage and thermal cycling. J Prosthet Dent 2004;91:356-62.

[17] Borges GA, Sophr AM, de Goes MF, Sobrinho LC, Chan DC. Effect of etching and airborne particle abrasion on the microstructure of different dental ceramics. J Prosthet Dent 2003;89:479-88.

[18] Brunton PA, Cattell P, Burke FJ, Wilson NH. Fracture resistance of teeth restored with onlays of three contemporary tooth-colored resin-bonded restorative materials. J Prosthet Dent 1999;82:167-71.

[19] Burns DR, Beck DA, Nelson SK. A review of selected dental literature on contemporary provisional fixed prosthodontic treatment: report of the Committee on Research in Fixed Prosthodontics of the Academy of Fixed Prosthodontics. J Prosthet Dent 2003;90:474-97.

[20] Cardoso MV, de Almeida Neves A, Mine A, Coutinho E, Van Landuyt K, De Munck J, Van Meerbeek B. Current aspects on bonding effectiveness and stability in adhesive dentistry. Aust Dent J 2011;56:31-44.

[21] Chaar MS, Passia N, Kern M. Ten-year clinical outcome of three-unit posterior FDPs made from a glass-infiltrated zirconia reinforced alumina ceramic (In-Ceram Zirconia). J Dent 2015;43:512-7.

[22] Clausen JO, Abou Tara M, Kern M. Dynamic fatigue and fracture resistance of non-retentive all-ceramic full-coverage molar restorations. Influence of ceramic material and preparation design. Dent Mater 2010;26:533-8.

[23] Coldea A, Swain MV, Thiel N. Mechanical properties of polymer-infiltrated-ceramic-network materials. Dent Mater 2013;29:419-26.

[24] Cronin RJ, Cagna DR. An update on fixed prosthodontics. J Am Dent Assoc 1997;128:425-36.

[25] De Munck J, Van Landuyt K, Peumans M, Poitevin A, Lambrechts P, Braem M, Van Meerbeek B. A critical review of the durability of adhesion to tooth tissue: methods and results. J Dent Res 2005;84:118-32.

[26] Della Bona A, Corazza PH, Zhang Y. Characterization of a polymer-infiltrated ceramic-network material. Dent Mater 2014;30:564-9.

[27] DeLong R, Douglas WH. Development of an artificial oral environment for the testing of dental restoratives: bi-axial force and movement control. J Dent Res 1983;62:32-6.

[28] Denry IL, Holloway JA. Microstructural and crystallographic surface changes after grinding zirconia-based dental ceramics. J Biomed Mater Res B Appl Biomater 2006;76:440-8.

[29] Dönmez MB, Yucel MT, Kilic I, Okutan Y. Novel ceramic primer vs. conventional treatment methods: Effects on roughness and bond strength of all-ceramic restorations. Am J Dent 2018;31:249-52.

[30] Edelhoff D, Beuer F, Schweiger J, Brix O, Stimmelmayr M, Güth JF. CAD/CAM-generated high-density polymer restorations for the pretreatment of complex cases: a case report. Quintessence Int 2012;43:457-67.

[31] Edelhoff D, Sorensen JA. Tooth structure removal associated with various preparation designs for posterior teeth. Int J Periodontics Restorative Dent 2002;22:241-9.

[32] Egilmez F, Ergun G, Cekic-Nagas I, Vallittu PK, Lassila LVJ. Does artificial aging affect mechanical properties of CAD/CAM composite materials. J Prosthodont Res 2018;62:65-74.

[33] El-Damanhoury HM, Gaintantzopoulou MD. Self-etching ceramic primer versus hydrofluoric acid etching: Etching efficacy and bonding performance. J Prosthodont Res 2017;62:75-83.

[34] Elsaka SE, Elnaghy AM. Mechanical properties of zirconia reinforced lithium silicate glass-ceramic. Dent Mater 2016;32:908-14.

[35] Erickson RL, Barkmeier WW, Kimmes NS. Bond strength of self-etch adhesives to pre-etched enamel. Dent Mater 2009;25:1187-94.

[36] Ferracane JL. Resin composite--state of the art. Dent Mater 2011;27:29-38.

[37] Fløystrand F, Kleven E, Oilo G. A novel miniature bite force recorder and its clinical application. Acta Odontol Scand 1982;40:209-14.

[38] Guazzato M, Albakry M, Ringer SP, Swain MV. Strength, fracture toughness and microstructure of a selection of all-ceramic materials. Part I. Pressable and alumina glass-infiltrated ceramics. Dent Mater 2004;20:441-8.

[39] Guess PC, Schultheis S, Wolkewitz M, Zhang Y, Strub JR. Influence of preparation design and ceramic thicknesses on fracture resistance and failure modes of premolar partial coverage restorations. J Prosthet Dent 2013;110:264-73.

[40] Guess PC, Stappert CF. Midterm results of a 5-year prospective clinical investigation of extended ceramic veneers. Dent Mater 2008;24:804-13.

[41] Güth JF, Almeida ESJS, Ramberger M, Beuer F, Edelhoff D. Treatment concept with CAD/CAM-fabricated high-density polymer temporary restorations. J Esthet Restor Dent 2012;24:310-8.

[42] He LH, Swain M. A novel polymer infiltrated ceramic dental material. Dent Mater 2011;27:527-34.

[43] Johnson AC, Versluis A, Tantbirojn D, Ahuja S. Fracture strength of CAD/CAM composite and composite-ceramic occlusal veneers. J Prosthodont Res 2014;58:107-14.

[44] Jongsma LA, Kleverlaan CJ, Feilzer AJ. Clinical success and survival of indirect resin composite crowns: results of a 3-year prospective study. Dent Mater 2012;28:952-60.

[45] Kelly JR. Perspectives on strength. Dent Mater 1995;11:103-10.

[46] Kern M, Douglas WH, Fechtig T, Strub JR, DeLong R. Fracture strength of all-porcelain, resin-bonded bridges after testing in an artificial oral environment. J Dent 1993;21:117-21.

[47] Kern M, Sasse M, Wolfart S. Ten-year outcome of three-unit fixed dental prostheses made from monolithic lithium disilicate ceramic. J Am Dent Assoc 2012;143:234-40.

[48] Kern M, Strub JR, Lü XY. Wear of composite resin veneering materials in a dual-axis chewing simulator. J Oral Rehabil 1999;26:372-8.

[49] Kern M, Thompson VP, Beuer F, Frankenberger R, Kohal RJ, Kunzelmann KH, Pospiech P, Reiss B. All-Ceramics at a Glance. 3rd ed. Ettlingen: Society for Dental Ceramics; 2017.

[50] Keul C, Martin A, Wimmer T, Roos M, Gernet W, Stawarczyk B. Tensile bond strength of PMMA-and composite-based CAD/CAM materials to luting cements after different conditioning methods. Int J Adhes Adhes 2013;46:122-7.

[51] Keul C, Müller-Hahl M, Eichberger M, Liebermann A, Roos M, Edelhoff D, Stawarczyk B. Impact of different adhesives on work of adhesion between CAD/CAM polymers and resin composite cements. J Dent 2014;42:1105-14.

[52] Kheradmandan S, Koutayas SO, Bernhard M, Strub JR. Fracture strength of four different types of anterior 3-unit bridges after thermo-mechanical fatigue in the dual-axis chewing simulator. J Oral Rehabil 2001;28:361-9.

[53] Khers SC, Carpenter CW, Vetter JD, Staley RN. Anatomy of cusps of posterior teeth and their fracture potential. J Prosthet Dent 1990;64:139-47.

[54] Kois DE, Isvilanonda V, Chaiyabutr Y, Kois JC. Evaluation of fracture resistance and failure risks of posterior partial coverage restorations. J Esthet Restor Dent 2013;25:110-22.

[55] Krämer N, Lohbauer U, Frankenberger R. Adhesive luting of indirect restorations. Am J Dent 2000;13:60-76.

[56] Lauvahutanon S, Takahashi H, Shiozawa M, Iwasaki N, Asakawa Y, Oki M, Finger WJ, Arksornnukit M. Mechanical properties of composite resin blocks for CAD/CAM. Dent Mater J 2014;33:705-10.

[57] Lawn BR, Deng Y, Miranda P, Pajares A, Chai H, Kim DK. Overview: damage in brittle layer structures from concentrated loads. J Mater Res 2002;17:3019-36.

[58] Lawson NC, Bansal R, Burgess JO. Wear, strength, modulus and hardness of CAD/CAM restorative materials. Dent Mater 2016;32:275-83.

[59] Lehmann F, Kern M. Durability of resin bonding to zirconia ceramic using different primers. J Adhes Dent 2009;11:479-83.

[60] Lin J, Kern M, Ge J, Zhu J, Wang H, Vollrath O, Mehl C. Influence of peripheral enamel bonding and chlorhexidine pretreatment on resin bonding to dentin. J Adhes Dent 2013;15:351-9.

[61] Lyann SK, Takagaki T, Nikaido T, Uo M, Ikeda M, Sadr A, Tagami J. Effect of different surface treatments on the tensile bond strength to lithium disilicate glass ceramics. J Adhes Dent 2018;20:261-8.

[62] Ma L, Guess PC, Zhang Y. Load-bearing properties of minimal-invasive monolithic lithium disilicate and zirconia occlusal onlays: finite element and theoretical analyses. Dent Mater 2013;29:742-51.

[63] Magne P, Schlichting LH, Maia HP, Baratieri LN. In vitro fatigue resistance of CAD/CAM composite resin and ceramic posterior occlusal veneers. J Prosthet Dent 2010;104:149-57.

[64] Magne P, Stanley K, Schlichting LH. Modeling of ultrathin occlusal veneers. Dent Mater 2012;28:777-82.

[65] Manhart J, Chen H, Hamm G, Hickel R. Buonocore Memorial Lecture. Review of the clinical survival of direct and indirect restorations in posterior teeth of the permanent dentition. Oper Dent 2004;29:481-508.

[66] Miyazaki T, Hotta Y, Kunii J, Kuriyama S, Tamaki Y. A review of dental CAD/CAM: current status and future perspectives from 20 years of experience. Dent Mater J 2009;28:44-56.

[67] Miyazaki T, Nakamura T, Matsumura H, Ban S, Kobayashi T. Current status of zirconia restoration. J Prosthodont Res 2013;57:236-61.

[68] Mörmann WH, Stawarczyk B, Ender A, Sener B, Attin T, Mehl A. Wear characteristics of current aesthetic dental restorative CAD/CAM materials: two-body wear, gloss retention, roughness and Martens hardness. J Mech Behav Biomed Mater 2013;20:113-25.

[69] Muts EJ, van Pelt H, Edelhoff D, Krejci I, Cune M. Tooth wear: a systematic review of treatment options. J Prosthet Dent 2014;112:752-9.

[70] Neumann P. CAD/CAM--ceramics an overview for the Cerec practitioner. Int J Comput Dent 1999;2:45-57.

[71] Oh SC, Dong JK, Lüthy H, Schärer P. Strength and microstructure of IPS Empress 2 glass-ceramic after different treatments. Int J Prosthodont 2000;13:468-72.

[72] Öztürk E, Bolay S, Hickel R, Ilie N. Shear bond strength of porcelain laminate veneers to enamel, dentine and enamel-dentine complex bonded with different adhesive luting systems. J Dent 2013;41:97-105.

[73] Peumans M, Van Meerbeek B, Lambrechts P, Vanherle G. Porcelain veneers: a review of the literature. J Dent 2000;28:163-77.

[74] Piemjai M, Arksornnukit M. Compressive fracture resistance of porcelain laminates bonded to enamel or dentin with four adhesive systems. J Prosthodont 2007;16:457-64.

[75] Poiate IA, de Vasconcellos AB, de Santana RB, Poiate E. Three-dimensional stress distribution in the human periodontal ligament in masticatory, parafunctional, and trauma loads: finite element analysis. J Periodontol 2009;80:1859-67.

[76] Preis V, Dowerk T, Behr M, Kolbeck C, Rosentritt M. Influence of cusp inclination and curvature on the in vitro failure and fracture resistance of veneered zirconia crowns. Clin Oral Investig 2014;18:891-900.

[77] Ramesh Kumar KR, Shanta Sundari KK, Venkatesan A, Chandrasekar S. Depth of resin penetration into enamel with 3 types of enamel conditioning methods: a confocal microscopic study. Am J Orthod Dentofacial Orthop 2011;140:479-85.

[78] Rammelsberg P, Spiegl K, Eickemeyer G, Schmitter M. Clinical performance of metal-free polymer crowns after 3 years in service. J Dent 2005;33:517-23.

[79] Rios D, Honorio HM, Francisconi LF, Magalhaes AC, de Andrade Moreira Machado MA, Buzalaf MA. In situ effect of an erosive challenge on different restorative materials and on enamel adjacent to these materials. J Dent 2008;36:152-7.

[80] Rosenblum MA, Schulman A. A review of all-ceramic restorations. J Am Dent Assoc 1997;128:297-307.

[81] Rueggeberg FA. Substrate for adhesion testing to tooth structure. Review of the literature. Dent Mater J 1991;7:2-10.

[82] Sasse M, Krummel A, Klosa K, Kern M. Influence of restoration thickness and dental bonding surface on the fracture resistance of full-coverage occlusal veneers made from lithium disilicate ceramic. Dent Mater 2015;31:907-15.

[83] Schenke F, Federlin M, Hiller KA, Moder D, Schmalz G. Controlled, prospective, randomized, clinical evaluation of partial ceramic crowns inserted with RelyX Unicem with or without selective enamel etching. Results after 2 years. Clin Oral Investig 2012;16:451-61.

[84] Schlichting LH, Maia HP, Baratieri LN, Magne P. Novel-design ultra-thin CAD/CAM composite resin and ceramic occlusal veneers for the treatment of severe dental erosion. J Prosthet Dent 2011;105:217-26.

[85] Schmalz G, Arenholt-Bindslev D. Biocompatibility of dental materials. Berlin Heidelberg: Springer; 2009.

[86] Schmidt KK, Chiayabutr Y, Phillips KM, Kois JC. Influence of preparation design and existing condition of tooth structure on load to failure of ceramic laminate veneers. J Prosthet Dent 2011;105:374-82.

[87] Sheets JL, Wilcox CW, Barkmeier WW, Nunn ME. The effect of phosphoric acid pre-etching and thermocycling on self-etching adhesive enamel bonding. J Prosthet Dent 2012;107:102-8.

[88] Shor A, Nicholls JI, Phillips KM, Libman WJ. Fatigue load of teeth restored with bonded direct composite and indirect ceramic inlays in MOD class II cavity preparations. Int J Prosthodont 2003;16:64-9.

[89] Soares CJ, Pizi EC, Fonseca RB, Martins LR. Influence of root embedment material and periodontal ligament simulation on fracture resistance tests. Braz Oral Res 2005;19:11-6.

[90] Sornsuwan T, Ellakwa A, Swain MV. Occlusal geometrical considerations in all-ceramic pre-molar crown failure testing. Dent Mater 2011;27:1127-34.

[91] Souza-Junior EJ, Prieto LT, Araujo CT, Paulillo LA. Selective enamel etching: effect on marginal adaptation of self-etch LED-cured bond systems in aged Class I composite restorations. Oper Dent 2012;37:195-204.

[92] Stawarczyk B, Basler T, Ender A, Roos M, Özcan M, Hämmerle C. Effect of surface conditioning with airborne-particle abrasion on the tensile strength of polymeric CAD/CAM crowns luted with self-adhesive and conventional resin cements. J Prosthet Dent 2012;107:94-101.

[93] Steiner M, Mitsias ME, Ludwig K, Kern M. In vitro evaluation of a mechanical testing chewing simulator. Dent Mater 2009;25:494-9.

[94] Tsitrou EA, van Noort R. Minimal preparation designs for single posterior indirect prostheses with the use of the Cerec system. Int J Comput Dent 2008;11:227-40.

[95] Van Landuyt KL, Kanumilli P, De Munck J, Peumans M, Lambrechts P, Van Meerbeek B. Bond strength of a mild self-etch adhesive with and without prior acid-etching. J Dent 2006;34:77-85.

[96] Wille S, Lehmann F, Kern M. Durability of resin bonding to lithium disilicate and zirconia ceramic using a self-etching primer. J Adhes Dent 2017;19:491-6.

[97] Yazigi C, Kern M, Chaar MS. Influence of various bonding techniques on the fracture strength of thin CAD/CAM-fabricated occlusal glass-ceramic veneers. J Mech Behav Biomed Mater 2017;75:504-11.

[98] Yildiz C, Vanlioglu BA, Evren B, Uludamar A, Kulak-Ozkan Y. Fracture resistance of manually and CAD/CAM manufactured ceramic onlays. J Prosthodont 2013;22:537-42.

[99] Zhang Y, Kim JW, Bhowmick S, Thompson VP, Rekow ED. Competition of fracture mechanisms in monolithic dental ceramics: flat model systems. J Biomed Mater Res B Appl Biomater 2009;88:402-11.

[100] Zhao K, Wei YR, Pan Y, Zhang XP, Swain MV, Guess PC. Influence of veneer and cyclic loading on failure behavior of lithium disilicate glass-ceramic molar crowns. Dent Mater 2014;30:164-71.

10. AKNOWLEDGEMENT

It is a great honor to express my sincere gratitude and appreciation to Prof. Dr. Matthias Kern, chairman of the Department of Prosthodontics, Propaedeutics and Dental Materials, Christian-Albrechts University at Kiel, for his valuable guidance, scientific supervision, and for all the time he gave me to make this thesis possible.

I take the opportunity to send my honest thankful to Dr. Mohamed Sad Chaar, senior lecturer in the Department of Prosthodontics, Propaedeutics and Dental Materials, Christian-Albrechts University at Kiel, for his kind suggestions, counseling, cooperation, and scientific supervision during this study.

I would like to thank all staff members at the Department of Prosthodontics, Propaedeutics and Dental Materials, Christian-Albrechts University at Kiel who helped me. In particular I would like to express my gratitude to Dr. Adham Elsayed for helping with the experiments, Dr. Abdulaziz Samran for collecting the natural teeth, Dr. Sebastian Wille for his consultation, Dipl-Ing. Frank Lehmann for his guidance and helpful discussion, Mr. Detlev Gostomsky for helping with documentation, and Mr. Rüdiger Möller for helping with the chewing simulator. Also, I am deeply thankful to Mrs. Eglal Al-Dobaei for her unlimited support during the preparation of this work; Dr. Shadi El Bahra and Dr. Shurouk Ali for their encouragement and support.

I would also like to thank Mr. Reinhard Busch head of the dental laboratory as well as his great team: Mr. Raphael Gerhardt, for his help in manufacturing the restorations, Mr. Carsten Radzinski and Mrs. Britta Schlüter for sharing their expertise with me.

Finally, I would like to gratefully acknowledge Ivoclar Vivadent AG, Schaan, Liechtenstein, and Vita Zahnfabrik, Bad Säckingen, Germany for donating the study materials.

11. DEDICATION

This doctorate thesis dedicated to my beloved mother, father, wife, brothers, sisters, my smart kids, and all my friends.

Thank you my family for your constant support, love, and encouragement for me to complete this Doctorate's program and make this thesis possible.

12. APPENDIXES

Fracture strength and failure mode of group LD-SE-0					
Description	**Fracture strength [N]**	**Failure mode**			
		I	**II**	**III**	**IV**
Lithium Disilicate + self-etching + without thermomechanical loading	821			III	
	850	I		III	
	848	I		III	
	744	I		III	
	1,210	I		III	
	712			III	
	678	I		III	
	586			III	
Mean	**806.13**				
±SD	**186.93**	38%	0%	62%	0%
Median	**782.50**				
First quartile	**686.5**				
Third quartile	**849.5**				

Fracture strength and failure mode of group LD-SE-1					
Description	**Fracture strength [N]**	**Failure mode**			
		I	**II**	**III**	**IV**
Lithium Disilicate + self-etching + after thermomechanical loading	1,070	I		III	
	98			III	
	1,010	I	II	III	
	98			III	
	98			III	
	98			III	
	559			III	
	735	I	II	III	
Mean	**470.75**				
±SD	**428.17**	23%	15%	62%	0%
Median	**328.50**				
First quartile	**98**				
Third quartile	**941.3**				

Note: The failed specimens in the fatigue test fractured under a load of 98 N. Therefore, their fracture strength was reported as 98 N rather than 0 N or excluded from the statistical analysis (98 N was the applied vertical load during the dynamic loading).

Fracture strength and failure mode of group LD-E&R-0					
Description	**Fracture strength [N]**	**Failure mode**			
		I	**II**	**III**	**IV**
Lithium Disilicate + etch-and-rinse + without thermomechanical loading	1,310	I		III	
	1,190	I			IV
	1,360	I		III	
	1,730	I	II	III	
	1,560	I	II	III	
	1,310	I	II	III	
	1,660	I		III	
	1,150	I			IV
Mean	**1,408.8**				
±SD	**215.8**	42%	16%	32%	10%
Median	**1,335**				
First quartile	**1,220**				
Third quartile	**1,635**				

Fracture strength and failure mode of group LD-E&R-1					
Description	**Fracture strength [N]**	**Failure mode**			
		I	**II**	**III**	**IV**
Lithium Disilicate + etch-and-rinse + after thermomechanical loading	1,360	I		III	
	1,300	I	II	III	
	1,770	I	II		IV
	1,410	I	II	III	
	1,700	I	II	III	
	1,520	I	II	III	
	1,700	I	II		IV
	1,600	I	II	III	
Mean	**1,545**				
±SD	**175.2**	35%	30%	26%	9%
Median	**1,560**				
First quartile	**1,372.5**				
Third quartile	**1,700**				

Fracture strength and failure mode of group LS-SE-0					
Description	**Fracture strength [N]**	**Failure mode**			
		I	**II**	**III**	**IV**
Zirconia-reinforced lithium silicate + self-etching + without thermomechanical loading	645	I	II	III	
	737	I	II	III	
	661	I		III	
	579			III	
	869	I	II	III	
	605			III	
	700			III	
	676	I	II	III	
Mean	**684**				
±SD	**90**	29%	24%	47%	0%
Median	**668.5**				
First quartile	**615**				
Third quartile	**727.8**				

Fracture strength and failure mode of group LS-SE-1					
Description	**Fracture strength [N]**	**Failure mode**			
		I	**II**	**III**	**IV**
Zirconia-reinforced lithium silicate + self-etching + after thermomechanical loading	1,020	I			
	98	I	II	III	
	842	I	II	III	
	98			III	
	1,250	I	II	III	
	98			III	
	983	I	II	III	
	921			III	
Mean	**663.8**				
±SD	**482.7**	31%	25%	44%	0%
Median	**881.5**				
First quartile	**98**				
Third quartile	**1,010.8**				

Fracture strength and failure mode of group LS-E&R-0					
Description	**Fracture strength [N]**	**Failure mode**			
		I	**II**	**III**	**IV**
Zirconia-reinforced lithium silicate + etch-and-rinse + without thermomechanical loading	1,670	I	II	III	
	1,240	I	II	III	
	1,300	I		III	
	1,010	I		III	
	958	I		III	
	616	I			
	1,020	I		III	
	800	I		III	
Mean	**1,076.8**				
±SD	**325**	47%	12%	41%	0%
Median	**1,015**				
First quartile	**839.5**				
Third quartile	**1,285**				

Fracture strength and failure mode of group LS-E&R-1					
Description	**Fracture strength [N]**	**Failure mode**			
		I	**II**	**III**	**IV**
Zirconia-reinforced lithium silicate + etch-and-rinse + after thermomechanical loading	1,760	I	II	III	IV
	1,510	I	II	III	
	1,790	I		III	IV
	1,360	I		III	
	1,860	I	II	III	IV
	1,860	I	II	III	IV
	1,490	I	II	III	
	1,710	I	II	III	
Mean	**1,667.5**				
±SD	**189.1**	31%	23%	31%	15%
Median	**1,735**				
First quartile	**1,495**				
Third quartile	**1,842.5**				

Fracture strength and failure mode of group PI-SE-0					
Description	**Fracture strength [N]**	**Failure mode**			
		I	**II**	**III**	**IV**
Polymer-infiltrated ceramic + self-etching + without thermomechanical loading	565			III	
	810	I		III	
	662			III	
	729	I		III	
	975	I	II	III	
	819	I		III	
	694	I		III	
	883	I		III	
Mean	**767.1**				
±SD	**130.9**	40%	7%	53%	0%
Median	**769.5**				
First quartile	**670**				
Third quartile	**867**				

Fracture strength and failure mode of group PI-SE-1					
Description	**Fracture strength [N]**	**Failure mode**			
		I	**II**	**III**	**IV**
Polymer-infiltrated ceramic + self-etching + after thermomechanical loading	861	I	II	III	
	696	I		III	
	98			III	
	752	I		III	
	98			III	
	98			III	
	98			III	
	98			III	
Mean	**349.9**				
±SD	**350.5**	25%	8%	67%	0%
Median	**98**				
First quartile	**98**				
Third quartile	**738**				

Fracture strength and failure mode of group PI-E&R-0					
Description	**Fracture strength [N]**	**Failure mode**			
		I	**II**	**III**	**IV**
Polymer-infiltrated ceramic + etch-and-rinse + without thermomechanical loading	832	I		III	
	1,000			III	
	798	I	II	III	
	1,170	I		III	
	958	I	II	III	
	1,010			III	
	1,190	I		III	
	1,190	I		III	
Mean	**1,018.5**				
±SD	**155.5**	38%	12%	50%	0%
Median	**1,005**				
First quartile	**863.5**				
Third quartile	**1,185**				

Fracture strength and failure mode of group PI-E&R-1					
Description	**Fracture strength [N]**	**Failure mode**			
		I	**II**	**III**	**IV**
Polymer-infiltrated ceramic + etch-and-rinse + after thermomechanical loading	1,170	I	II	III	IV
	1,590	I		III	
	1,290	I	II	III	
	848	I		III	
	1,500	I		III	
	1,160			III	
	1,680			III	
	1,330	I		III	
Mean	**1,321**				
±SD	**269.1**	35%	12%	47%	6%
Median	**1,310**				
First quartile	**1,162,5**				
Third quartile	**1,567.5**				

Fracture strength and failure mode of group PM-SE-0					
Description	**Fracture strength [N]**	**Failure mode**			
		I	**II**	**III**	**IV**
Polymethylmethacrylate + self-etching + without thermomechanical loading	1,020	I		III	
	722	I		III	
	1,030	I	II	III	
	939	I		III	
	634	I	II	III	
	1,120	I		III	
	835	I		III	
	880	I		III	
Mean	**897.5**				
±SD	**164**	44%	11%	45%	0%
Median	**909.5**				
First quartile	**750.3**				
Third quartile	**1,027.5**				

Fracture strength and failure mode of group PM-SE-1					
Description	**Fracture strength [N]**	**Failure mode**			
		I	**II**	**III**	**IV**
Polymethylmethacrylate + self-etching + after thermomechanical loading	98			III	
	770	I		III	
	855	I		III	
	791	I		III	
	888	I		III	
	98			III	
	98			III	
	98			III	
Mean	**462**				
±SD	**390.8**	33%	0%	67%	0%
Median	**434**				
First quartile	**98**				
Third quartile	**839**				

Fracture strength and failure mode of group PM-E&R-0					
Description	**Fracture strength [N]**	**Failure mode**			
		I	**II**	**III**	**IV**
Polymethylmethacrylate + etch-and-rinse + without thermomechanical loading	1,031	I		III	
	593	I		III	
	814	I		III	
	1,010	I		III	
	978			III	
	940	I		III	
	1,140			III	
	1,290	I		III	
Mean	**974.5**				
±SD	**208.4**	43%	0%	57%	0%
Median	**994**				
First quartile	**845.5**				
Third quartile	**1,112.8**				

Fracture strength and failure mode of group PM-E&R-1					
Description	**Fracture strength [N]**	**Failure mode**			
		I	**II**	**III**	**IV**
Polymethylmethacrylate + etch-and-rinse + after thermomechanical loading	1,520	I		III	
	1,010	I		III	
	1,430	I		III	
	1,150			III	
	1,100	I		III	
	1,110	I		III	
	1,530	I		III	
	1,010			III	
Mean	**1,232.5**				
±SD	**223.1**	43%	0%	57%	0%
Median	**1,130**				
First quartile	**1,032.5**				
Third quartile	**1,497.5**				